

Review

Hydrothermal Carbonization as a Valuable Tool for Energy and Environmental Applications: A Review

Manfredi Picciotto Maniscalco, Maurizio Volpe  and Antonio Messineo * 

Faculty of Engineering and Architecture, Kore University of Enna, Cittadella Universitaria, 94100 Enna, Italy; manfredi.maniscalco@unikore.it (M.P.M.); maurizio.volpe@unikore.it (M.V.)

* Correspondence: antonio.messineo@unikore.it

Received: 6 July 2020; Accepted: 4 August 2020; Published: 7 August 2020



Abstract: Hydrothermal carbonization (HTC) represents an efficient and valuable pre-treatment technology to convert waste biomass into highly dense carbonaceous materials that could be used in a wide range of applications between energy, environment, soil improvement and nutrients recovery fields. HTC converts residual organic materials into a solid high energy dense material (hydrochar) and a liquid residue where the most volatile and oxygenated compounds (mainly furans and organic acids) concentrate during reaction. Pristine hydrochar is mainly used for direct combustion, to generate heat or electricity, but highly porous carbonaceous media for energy storage or for adsorption of pollutants applications can be also obtained through a further activation stage. HTC process can be used to enhance recovery of nutrients as nitrogen and phosphorous in particular and can be used as soil conditioner, to favor plant growth and mitigate desertification of soils. The present review proposes an outlook of the several possible applications of hydrochar produced from any sort of waste biomass sources. For each of the applications proposed, the main operative parameters that mostly affect the hydrochar properties and characteristics are highlighted, in order to match the needs for the specific application.

Keywords: HTC; waste biomass; energy recovery; environmental remediation; nutrients recovery; activated carbon

1. Introduction

The increasing need of finding new renewable energy alternatives to fossil fuels together with the need to safely dispose of organic waste has pushed, in the last few years, the investigation for more efficient and reliable technologies for waste biomass energy exploitation and conversion towards valuable materials. Indeed, the constant rise in the global energy consumption together with the parallel decrease in the fossil fuel reservoirs, has driven the scientific community toward the research of more sustainable sources [1]. Waste biomass, and in particular the organic fraction of municipal solid waste (OFMSW) and industrial and sewage sludges are among the most studied residual feedstocks to produce energy and valuable carbonaceous materials [2–6].

One of the major drawbacks of choosing waste biomass for energy production, is the need for one or more pre-treatments before use [7]. The low energy density due to the high moisture content of waste biomass, makes it often not suitable for a direct energy conversion by combustion and/or gasification [8–10]. The high moisture in residual biomass raises significantly the operational cost of transportation and energy consumption for drying [11]. However, due to its great abundance, globally availability, carbon neutrality and the necessity to find efficient and valuable technologies to treat and convert it into sustainable energy sources and exploitable materials, waste biomass has gained increasing attention and investigation [12].

Between different valuable alternative treatments for waste biomass, wet thermochemical technologies for their flexibility and, principle, their low investment and operating costs are receiving increasing attention in the last years [13,14]. In particular, hydrothermal carbonization (HTC), also known as wet pyrolysis, is a thermochemical process performed in the presence of sub-critical water at temperature usually between 180 and 280 °C and autogenous saturated vapor conditions (10–80 bars). Residence time is varied from minutes up to several hours [3,15,16]. At high temperature and pressure, even at subcritical conditions, water undergoes a dramatic properties change acting more as an organic solvent and its increased ion product favors reactions that are typically catalyzed by acids or bases, promoting biomass decomposition through hydrolysis, dehydration and decarboxylation reactions [17,18]. By means of these reactions, it is possible to increase the carbon content of the initial feedstock, by removing most of the more volatile oxygenated compounds (furans and low molecular fatty acids) that are typically moved to the aqueous phase [19]. It is also well documented in the literature that, during HTC, part of the inorganics are moved to the liquid phase [19–21] thus, on the one hand, reducing in the solid residue (hydrochar), minerals and ash formation during combustion, and on the other hand, increasing the high heating values (HHV) [17,22]. This behavior leads to a reduced risk of slugging and fouling phenomena during combustion of hydrochars in boilers if compared to the use of pyrochars [2,23,24]. Hydrochar can be used in numerous applications, as a bio fuel for energy production [1,13,25], as a source of carbon and nutrients in soil application [19,26,27] or even as starting material for further advanced utilization in supercapacitors or a porous matrix for the adsorption of pollutants [28,29]. Moreover, the possible scalability of the process up to the industrial level [30], as well as relatively mild process conditions, make HTC a valid solution for the near future for the transformation of a wide range of raw biomass into valuable materials [13,30]. In Figure 1 is reported a flowchart of hydrochar production from waste biomass and its possible energetic and environmental applications.

Since HTC is performed under wet conditions, this technology can find its best application for biomasses that present high initial moisture content. Indeed, when dealing with direct combustion, a detrimental overall efficiency was shown when the starting biomass presents high moisture content [10]. The main reaction pathways involved in the hydrothermal carbonization process are still under discussion among the scientific community [31]. One possible route was discussed by Jatzwauck and Schumpe [32], according to which the HTC process is essentially divided into three steps. The first one is mainly related to the hydrolyzation of cellulose, hemicellulose and part of the lignin. During the second step, the generated intermediates endure further re-arrangement resulting in the generation of gaseous products. As an alternative to the formation of the gas phase, intermediate products can conglomerate to form secondary char, during the third step. The other mostly discussed route, regarding the evolution of HTC reactions, involves two main pathways: a solid–solid transformation, according to which hydrochar is directly generated from the dehydration of the initial biomass, and a vapor–solid reaction in which the dissolved organics present in the solution, back polymerize to form again a solid material, often named coke or secondary char [33–35].

The present work attempted to review the most relevant research on HTC of the last 5 years, in order to derive the best operative conditions for the production of valuable hydrochar materials. Moreover, whenever possible, the present review was integrated with a further pyrolysis or gasification process in order to evaluate how HTC behaves as a thermo-chemical pre-treatment for the production of porous material or precursor for energy application purposes.



Figure 1. Waste biomass hydrochar potential applications.

2. Effect of HTC Operating Conditions

It is well established that the HTC treatment induces some major transformations inside the biomass particles, in accordance with the severity of the process that is performed. From an operative point of view, the three main parameters that can be varied in a HTC process are temperature, residence time and biomass-to-water ratio. It was found that each of these variables can differently influence the intermediate reaction and the output products in terms of yields and composition [33,36]. The evolution of the main biomass components (lignin, cellulose and hemicellulose) in relation to the reaction severity was recently studied and modelled [37,38]. Heidari et al. [37] found almost negligible interactions between lignin, cellulose and hemicellulose on the final hydrochar properties, while cellulose was mostly affected by reaction severity. Authors also conducted an evaluation on the optimal proportion between biomass components to increase carbon content and calorific value of hydrochar, finding that a cellulose, hemicellulose and lignin content respectively of 40%, 35% and 25%, represents the optimal starting conditions. Another main parameter that can significantly influence the composition of the final hydrochar is the origin of the biomass. It is well known that ligno-cellulosic biomass is mainly composed of lignin, cellulose and hemicellulose, but the extent of their proportion in the overall biomass composition is strictly related to the nature of the material considered. At the same time each of these components undergoes degradation processes at different extent in accordance to the process conditions [39,40]. The first component that is subjected to hydrolyzation is hemicellulose, which starts to degrade at temperatures of 180–200 °C [41], followed by cellulose depolymerization (above 210 °C) [40] and softening of lignin [42]. Complete conversion of hemicellulose for reaction temperature of 180 °C and residence time of 4 h was reported by Olszewski et al., when treating brewer's spent grains [43]. Cellulose was found to be the most difficult component to be degraded, as reported

by Titirici [31]. According to the author, cellulose starts to be converted above 210 °C according to two different pathways, as depicted in Figure 2 [31]. In their experiments, Olszewski et al. [43] and Volpe et al. [40] reported a complete cellulose conversion at a reaction temperature of 260 °C.

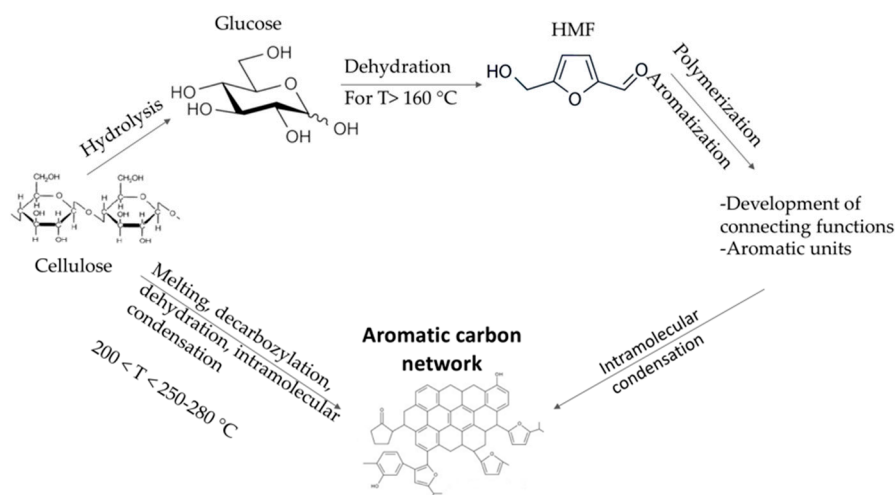


Figure 2. Cellulose conversion pathways, as proposed in Titirici, 2012.

Due to its very complex structure, lignin undergoes decomposition under a wider temperature range with respect to hemicellulose and cellulose [44]. The deterioration starts at around 200 °C, leading to the disruption of highly reactive alkyl-aryl-ether bonds, which further react with other intermediate compounds to form highly stable products [45]. Volpe et al. [19], when performing thermogravimetric analysis (TGA) on olive mill waste hydrochar, found that while cellulose peak is significantly reduced for HTC temperature of 250 °C, the peak associated to lignin increases [44]. Through the same analysis, authors also confirmed the production of lower molecular compounds and/or tarry products coming from the decomposition of lignin. Indeed, a new peak in TGA curve at around 250 °C was found for the sample produced at 220 and 250 °C. From these considerations, it can be deduced that different reaction temperatures lead to different compositions in terms of cellulose, hemicellulose and lignin. The study conducted by Kim et al. [46] reported the energy retention efficiency (ERE) for each of these components in relation to reaction temperature. Indeed, as previously reported, as HTC temperature is raised, the calorific value increases as well, but the mass yield is reduced. It is therefore of paramount importance to define the best conditions to maximize the ERE, in order to obtain a valuable biochar for energy purposes. The results of this study showed that ERE for lignin and cellulose was maximized, respectively, at 200 °C and 220 °C, while the best temperature for the conversion of biomass into high energetic medium appeared to be 220 °C.

The higher thermal stability of lignocellulosic against non-lignocellulosic biomass was also confirmed by Zhuang et al. [47], testing herb tea waste (lignocellulosic) and penicillin mycelial waste (non-lignocellulosic). The analysis performed on the hydrochars produced showed a superior thermal stability for the tea waste, due to the presence of hemicellulose and lignin which start to degrade above 210 °C, while polysaccharide and protein present in the penicillin mycelial waste were hydrolyzed at temperatures lower than 180 °C. Finally, some considerations should be addressed regarding the influence of pressure, particle size, and the possibility of water recirculation within the system. With respect to the first parameter, the autogenous pressure that is developed inside the reactor maintains the water in the liquid state, favoring its ability to dissolve polar compounds [48]. Higher pressure levels result in smaller hydrochar dimensions and higher pore volume, together with a mild increase in the HHV. Only when pressure is raised above 100 MPa, significant increases in the HHV can be achieved, but the higher cost of the reactor can limit the application [48]. Regarding particle size and water recirculation, Heidari et al. [49] found that when biomass dimension was raised from <0.25 mm to within the range of 1.25–3 mm, a slight increase in the mass yield was observed,

but the calorific value was lower. This condition is explained by the more severe conversion that biomass endures since water can more easily penetrate and reach the inner core of the biomass particle. Water recirculation affects almost only the mass yield, increasing it after the first recycle of about 12%, while the contribution to HHV is almost negligible, since it was raised by just 2%.

Proximate and ultimate analysis have been widely used to characterize the hydrochars properties. Proximate analysis is used to get an overall picture of the char composition in terms of fixed carbon (FC), volatile matter (VC), ash and moisture content (M), while the ultimate analysis give the weight percentages of their major elements (C, H, N, S, O). Although not all the reactions involved in HTC treatment are well known, the general evolution pathways of the main biomass elements are fairly well understood. As long as reaction severity is increased, most of the volatile compounds are released, increasing carbon content and heating value. The main reactions occurring are dehydration and de-hydrogenation which imply, respectively, the removal of hydroxyl groups and the rupture of the long chain carboxylic acids [50]. Different studies evaluated the effect of residence time and reaction temperature on the final hydrochar yields and properties [4,17,51,52]. The results of the studies assert that the main contribution to biomass degradation and increase in the calorific value is reaction temperature rather than residence time [53]. Lucian et al. [51] reported an increase in the heating value of olive trimming from 22.6 to 27.8 MJ kg⁻¹ when reaction temperature was raised from 180 to 250 °C. At the same time, increasing the residence time from 1 to 6 h led to a maximum increase in HHV of +2 MJ kg⁻¹, at the temperature of 220 °C, passing from 24.7 to 26.7 MJ kg⁻¹. The increase in the calorific value is mainly due to the combined effect of the removal of oxygen and volatile compounds and the parallel rise in carbon content. The evolution of the concentration of carbon, oxygen and hydrogen is usually represented through the van Krevelen diagram in H/C and O/C ratios which are plotted. It is fairly stated that an increase in the hydrothermal carbonization temperature boosts dehydration reactions, removing oxygen from the initial biomass structure, resulting in a decrease in the O/C ratio. The evolution of the hydrochar composition is represented in the van Krevelen diagram through a shift toward lower values of O/C, characteristic of highly carbonaceous fuels like lignite or coals. Ulbrich et al. stated that the removal of oxygen for low HTC temperature is only mildly affected by residence time, while in the temperature range of 230–280 °C a more pronounced connection between oxygen reduction and residence time was observed [52]. Figure 3 displays the van Krevelen diagrams for three biomass sources reported in the literature: a sugar rich waste, namely rotten apples and coming from the fruit industry, a lignocellulosic residue (olive trimming) and a protein based biomass (Penicillin mycelial waste) [1,51,54]. It can clearly be seen that each waste endures a specific evolution pathway, in relation to its initial structure and composition. Evidences of the different transformations that biomass endures during HTC, in relation to its origin process parameters, are reported in Table 1. Lignocellulosic material, like olive trimming, presents higher thermal stability than proteins and polysaccharides, resulting in higher mass yield (approx. 50%) and fixed carbon (9%) with respect to fruit and protein-based wastes.

Hydrochar produced from fruit wastes resulted in an increase in fixed carbon as long as reaction temperature is raised, due to the conversion of glucose which starts at around 225 °C [1]. Different research groups showed that mass yield is mainly affected by reaction temperature, rather than residence time. For low reaction temperature, residence time can even have a positive effect on the final mass yield. Chen et al. [55], as well as Lucian et al. [51], reported an increase in mass yield when reaction temperature was set respectively at 190 and 180 °C for a reaction time of 6 h, when compared to mass yields obtained at 1-h reaction time. The increase in hydrochar mass is associated with a re-arrangement and back polymerization of organic compounds from liquid to solid phase [55].

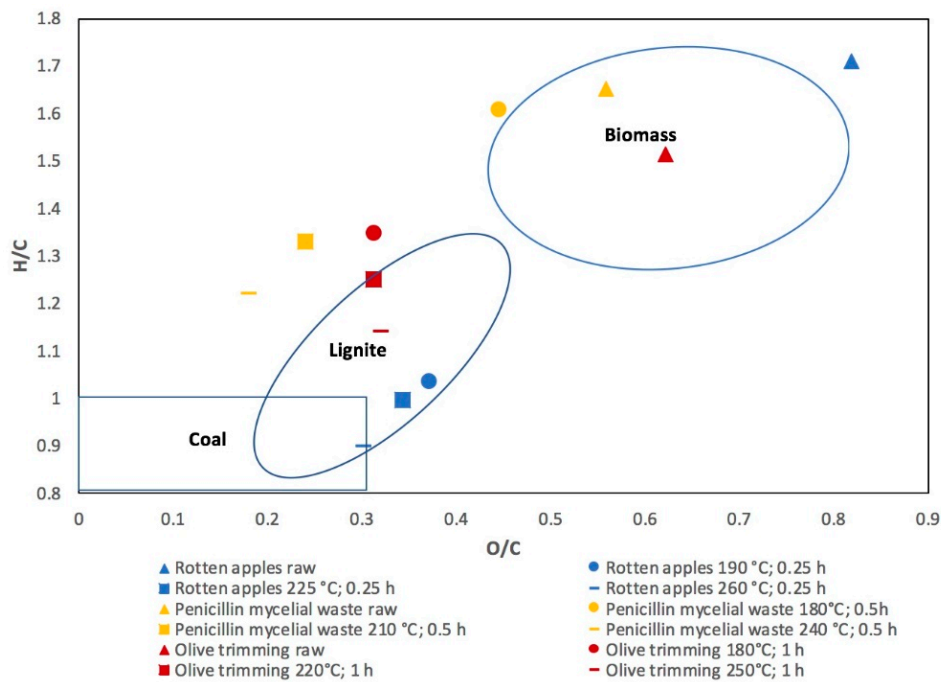


Figure 3. van Krevelen diagram of hydrothermal carbonization (HTC) treatment of rotten apples, Penicillin mycelial and olive trimming.

As previously reported, the last parameter that can be varied when performing HTC treatment is the biomass-to-water ratio (B/W). Volpe et al. [17] found that when biomass is increased in the mix up to a B/W ratio equal to 0.2, the share of secondary char production is increased as well, boosting the HHV of the hydrochar. In terms of ash content, HTC presents a huge advantage over other pre-treatment process such as pyrolysis. In fact, although during “dry” pre-treatment all the inorganics are kept inside the biomass structure, increasing their content in the final product due to the mass loss during the heating, in HTC some of the ash forming elements are removed from the biomass and washed away with the process water [24].

Table 1. Effect of HTC reaction parameters on hydrochar composition, calorific value and mass yield, together with coal properties as reference.

Biomass	FC [%]	VM [%]	C [%]	H [%]	O [%]	HHV _{raw} [MJ/kg]	HTC Temp [°C]	Res. Time [h]	FC _{HTC} [%]	VM _{HTC} [%]	C _{HTC} [%]	H _{HTC} [%]	O _{HTC} [%]	HHV _{HC} [MJ/kg]	MY [%]	Ash _{HC} [%]	Ref.
Pine	13.1	87.8	48.1	6.6	45.1	19.2	220	4.0	30.8	68.8	66.0	5.9	27.5	25.9	76	0.4	[56]
Straw	14.8	80.9	48.2	6.5	40.6	18.2	220	4.0	25.2	72.6	57.9	5.0	34.4	22.4	56	2.2	[56]
Herb tea waste	17.2	69.4	45.1	5.9	32.7	19.3	150	0.5	15.3	68.8	54.9	6.9	34.8	19.8	84	15.8	[54]
							180	0.5	16.0	65.8	58.6	6.9	31.6	20.5	69	18.1	
							210	0.5	16.6	63.4	62.6	6.9	27.6	22.1	63	20.0	
							240	0.5	19.1	58.4	68.4	6.5	22.1	26.3	53	22.5	
Penicillin mycelial waste	14.0	78.3	44.8	6.1	33.4	19.1	150	0.5	14.3	76.9	50.2	7.3	34.4	21.3	71	8.7	[54]
							180	0.5	15.9	73.6	53.3	7.1	31.6	23.6	38	10.5	
							210	0.5	17.1	68.2	64.5	7.1	20.6	27.4	29	14.6	
							240	0.5	18.9	63.8	69.2	7.0	16.5	29.2	23	17.2	
Sewage sludge	3.51	39.9	21.5	3.7	14.2	9.3	150	0.5	3.1	31.6	50.4	8.4	33.5	10.4	79	65.4	[54]
							180	0.5	2.8	24.7	57.1	8.3	27.2	10.2	75	72.5	
							210	0.5	2.4	19.6	66.4	9.4	16.7	8.1	72	77.9	
							240	0.5	2.2	16.8	71.5	9.9	11.0	7.7	68	81	
Brewer spent grains (80% moisture)	16	76.2	51.3	6.9	36.5	22.3	180	2.0	17.8	74.9	60.3	7.1	27.8	26.5	68	4.3	[4]
							200	2.0	20.8	71.9	62.0	7.0	26.4	27.2	64	4.3	
							220	2.0	23.7	69.0	65.8	7.3	22.1	29.2	58	4.3	
							180	4.0	26.7	72.8	62.9	7.0	25.2	27.6	67	4.2	
							200	4.0	23.0	70.5	61.2	7.1	27.2	26.9	63	4.1	
							220	4.0	29.6	66.2	67.1	6.9	21.1	29.3	55	4.2	
Brewer spent grains (90% moisture)	16	76.2	51.2	6.9	36.5	22.3	180	2.0	22.4	74.2	60.2	7.4	28.3	26.7	66	3.4	[4]
							200	2.0	25.1	71.7	62.3	7.2	26.2	27.5	62	3.2	
							220	2.0	28.7	68.0	66.5	7.3	21.9	29.6	52	3.2	
							180	4.0	23.7	73.1	59.9	7.0	29.1	26.2	65	3.1	
							200	4.0	26.5	70.3	63.5	7.2	24.9	28.0	60	3.2	
							220	4.0	31.9	64.8	66.6	6.9	21.8	29.1	51	3.3	
Rotten apples	14.8	83.6	43.5	6.2	47.5	17.5	190	0.25	34.2	65.5	62.4	5.4	30.8	24.8	36	0.3	[1]
							225	0.25	35.9	63.9	64.2	5.3	29.4	25.7	36	0.2	
							260	0.25	37.9	61.6	66.8	5.0	26.8	26.0	39	0.4	

Table 1. Cont.

Biomass	FC [%]	VM [%]	C [%]	H [%]	O [%]	HHV _{raw} [MJ/kg]	HTC Temp [°C]	Res. Time [h]	FC _{HTC} [%]	VM _{HTC} [%]	C _{HTC} [%]	H _{HTC} [%]	O _{HTC} [%]	HHV _{HC} [MJ/kg]	MY [%]	Ash _{HC} [%]	Ref.
Grape pomace	11.6	87.5	44.1	6.2	41.9	17.5	190	0.25	28.8	68.6	55.7	5.5	34.5	21.8	38	2.6	[1]
							225	0.25	35.4	62.8	61.4	5.1	29.9	24.5	40	1.7	
							260	0.25	35.0	60.6	64.9	5.0	24.9	24.8	45	4.3	
Peat moss	27.4	65.9	51.1	5.4	42.0	21.3	240	0.25	40.5	52.4	59.5	4.8	34.1	25.2	74	7.1	[57]
								0.5	42.4	51.4	61.5	5.0	31.8	25.3	73	6.2	
								0.75	41.8	51.5	62.1	4.9	31.3	25.8	70	6.8	
Olive trimming	17.6	78.4	48.3	6.1	40	19.8	180	1.0	20.3	76.1	54.3	6.1	34.3	22.6	72	3.5	[51]
							180	3.0	23.2	72.9	56.7	6.2	31.4	23.4	70	3.9	
							180	6.0	21.9	73.8	58.9	5.9	29.2	24.1	73	4.3	
							220	1.0	25.1	70.6	59.4	6.2	28.3	24.7	63	4.3	
							220	3.0	31.4	64.4	63.0	6.3	24.4	26.4	58	4.2	
							220	6.0	28.4	66.9	65.5	6.0	21.8	26.7	57	4.6	
							250	1.0	29.2	66.8	65.3	6.2	22.2	27.8	52	4.0	
250	3.0	35.7	59.6	68.9	6.3	17.6	29.0	48	4.7								
250	6.0	39.9	56.3	70.6	5.9	17.5	29.6	50	3.8								
Sub-bituminous Coal	35.1	33.1	60.8	5.7	15.6	28.2										8(*)	[58]

FC = fixed carbon; VM = volatile matter; MY = mass yield. (*) the value of ash for sub-bituminous coal is referred to the raw material and not the hydrothermally carbonized one.

3. HTC of Waste Biomass for Energy Production and Storage

Hydrothermal carbonization has been proven to be an effective tool for waste biomass pre-treatment, to produce highly carbonaceous materials that can be used for energetic applications [59–62]. In the last 5 years, research projects have focused their attention on the possible energetic use of the HTC products as a carbon-rich material for direct combustion or as a precursor for the realization of supercapacitors [63–66]. Prior to any of its further use, hydrochar must be dried to remove all the moisture.

3.1. Direct Combustion

Hydrochar has shown better energetic properties with respect to the raw original biomass. In fact, the increased heating value and the reduced volatile content ensure a better combustion and exploitation of the calorific properties of the biomass. Moreover, the lower ash content due to the removal in the liquid phase of part of the inorganics, reduce fouling and slagging phenomena that can lead to inefficacy and increased maintenance of the boiler [16,67,68].

Numerous studies investigated the possible use of hydrochar from HTC of sludge for direct combustion in a boiler. Most of the researches involve sludge from municipal waste water treatment plants, but recently also industrial sludge, like from a paper mill plant was proposed [69]. Merzari et al. studied the HTC as a strategy for sewage sludge management [70,71]. Peng et al. [72] tested various temperatures and residence times for the pre-treatment of sewage sludge from a waste water treatment plant, before its combustion. Temperature was varied in the range of 180–300 °C, with a 40 °C interval with a residence time of 30 min, while, to evaluate the contribution of reaction time authors kept the temperature fixed at 260 °C for 30, 60, 90, 360 and 480 min. Authors found that 260 °C and a residence time between 30 and 90 min, led to the highest increase in the higher heating value (2–10%). A further prolongation of reaction time up to 360 min, induced only an increment in the ash content up to 69.26%. The ash-related problems are common issues when dealing with sludges from waste water treatment plants. Wang et al. [73] studied the behavior of high-ash municipal sewage sludge when subjected to HTC in the temperature range of 170–350 °C. Raw sludge presented poor energetic properties, due to the very high ash and volatile matter (VM) content and the low fixed carbon amount. Similarly to what was reported previously by Peng et al. [72] and by Chen et al. [74], a mild HTC treatment with temperatures below 260 °C determines the best hydrochar properties for the further combustion stage. Indeed, the reduced ash content, the higher dewaterability and the greater HHV with respect to the other pre-treatment conditions, make this temperature the optimum one at which to process sludges. A valid practice to obtain hydrochar with better combustion performances, is to perform a co-HTC with carbon rich biomass, in order to raise the carbon content and the calorific value [57,75,76]. Zheng et al. [77] tested co-HTC of food waste (FW) and municipal sludges (MS) under different ratios and carbonization temperatures. The share of food waste in the mix was varied between 30, 50 and 70%, while the temperatures tested were 180 °C, 230 °C and 280 °C. The addition of food waste can partly mitigate the drawbacks related to poor combustion properties of sewage sludge hydrochar by raising the HHV and the carbon content, while lowering at the same time the ash amount. As long as the amount of food waste was raised in the feedstock mix, authors reported a drastic increase in the HHV which passed from 9.62 MJ kg⁻¹ for the hydrochar prepared at 230 °C from only MS to 19 and 23 MJ kg⁻¹ when the amount of FW was, respectively, 50 and 70%. At a temperature of 230 °C, HTC of only food waste produced a good quality solid fuel with a HHV of 31 MJ kg⁻¹ and an ash content of 6%. Another perspective on the possible use of food waste as feedstock for HTC conversion was presented by Wang et al. [78] and McGaughy et al. [79]. Wang et al. [78] found a similar trend in the evolution of the calorific value of the hydrochar, with a peak of 31.7 MJ kg⁻¹ when FW was treated at 260 °C for 1 h. In addition, fouling and slagging phenomena were reduced. Indeed, as long as reaction temperature increases, the removal of inorganics like Cl, S and N, together with a great share of alkali metals, is enhanced which contribute the most to slagging and fouling problems. However, when the carbonization temperature was raised above 220 °C, authors encountered an increased emission of NO_x, which should be avoided during combustion. McGaughy and Reza [79], on the basis of HTC

experiments with food waste, proposed a simulation model of a plant processing 1 ton of fresh refuse per day, resulting in a positive net energy balance for the whole process.

Food waste in the form of digestate from biogas plants, was experimented by Cao et al. [80]. The digestion significantly reduced the potential for energy conversion, since it converted a great share of the carbonaceous content to methane and carbon oxides and increased the ash amount with respect to the raw material. HTC treatment did not show significant improvement in terms of combustion potential. Poor energetic properties were also reported in [81] when dealing with the wet fraction of municipal solid waste digestate, but mostly due to the scarce potential of the initial feedstock.

A good potential for solid fuel conversion was proposed in [82,83] for the lignocellulosic material. In [82] authors tested the efficacy of a 220 °C, 90 min HTC treatment on six different biomasses, namely: olive pomace, walnut shell, hazelnut shell, apricot seed, tea stalk and wood sawdust. Each of the biomasses studied, presented better combustion properties with respect to the initial feedstock, in terms of heating value, carbon content and ignition conditions. The best energetic properties were found to be related to the olive pomace with an increase in the HHV of up to 25.6 MJ kg⁻¹ and an ash content of 5.5%, while hazelnut husks showed the poorest properties with a HHV of 20.6 MJ kg⁻¹ and an ash percentage of approximately 12%. Moreover, all the hydrochar presented higher ignition temperatures with respect to the raw biomasses, which significantly improve the handling and storage properties of the fuels, reducing the risk of self-ignition and combustion. Similar properties of the obtained hydrochar were also reported by Chen et al. when dealing with HTC of sweet potato peels [84].

3.2. Supercapacitors & Batteries Application

The research on possible use of biomass-derived material as source for electrode fabrication has recently increased the attention on the use of HTC pre-treatment. The present review will consider only the methods involving the use of waste biomass as starting material. This consideration is due to the fact that some studies had focused the attention mostly on the activation step, using synthesized glucose or lignin as starting material, while in the present work only the biomass-derived precursors were considered. Agricultural wastes, as well as plant wastes or high lignocellulosic materials were reported as suitable for energy storage applications [85–88]. Application for supercapacitors has been more and more studied in recent years. Supercapacitors can deliver great power output, ensuring at the same time long life and great efficiency after hundreds of cycles [86]. Supercapacitors store charge reversibly through ions immobilization in the electric double layer, on which non-faradaic and pseudocapacitive reaction occurs [87]. Hence, carbon-based material for supercapacitors applications must ensure good electric conductivity, great surface area with possible hierarchical pore distribution, together with a reasonable cost. For such reason, biomass material represents a greatly attractive option in this field [87].

Soybean root was tested by Guo et al. [89], resulting in a great electrode capacitance and cycling stability. Authors performed an acid HTC treatment at 180 °C for 18 h by using a 5% *w/w* H₂SO₄ solution. The obtained hydrochars were further active with KOH at 800 °C for 3 h, under a N₂ atmosphere. The Brunauer–Emmet–Teller (BET) and Scanning Electron Microscope (SEM) analysis showed the formation of a hierarchical interconnected porous structure composed of large macro and meso-pores on the external surface, which further develop into a capillary net of micropore sites. These latter spots are the ones that mainly contribute to ions storage [90]. Cyclic voltammetry (CV) showed great electrical response even at a high scanning rate, reporting an almost rectangular trend of the curve even at 800 mV s⁻¹, as well as a significant capacitance of 328 F g⁻¹ for a current density of 1 A g⁻¹.

Tests on bamboo shells were reported by [65], resulting in a lower capacitance with respect to the ones reported by Gou et al. [89], and equal to 209 F g⁻¹ at 0.5 A g⁻¹. Similarly in this case, authors performed an acid HTC treatment with 1% *w/w* H₂SO₄ solution and the obtained hydrochars, before being activated in KOH at 600–800 °C, were carbonized with melamine under N₂ at a temperature of 600 °C, with a char-to-melamine ratio of 1:4 *w/w*. To better understand the effect of melamine

treatment on the final product, a blank assay was also conducted. The results showed a remarkable increase in surface area and pore development, as well as in the capacitance properties of the hydrochar. Melamine for hydrochar activation was also studied by Sevilla et al. [91], mixing it with $K_2C_2O_4$ and the hydrochar obtained from eucalyptus sawdust produced at 250 °C for 4 h. The use of $K_2C_2O_4$, instead of the more frequently used potassium hydroxide, according to the authors, is due to three main reasons: its lower corrosive potential, the higher obtainable product yield and its less disruptive action on the morphology of chars. The use of $K_2C_2O_4$ instead of KOH can almost double the char production, for the same amount of reactant adopted, while increasing at the same time the electrical properties. Hydrochar from pine cones, hemp waste, tobacco rods, peony pollen and argy worm-wood were successfully tested as precursors for supercapacitors application through KOH activation [63,92–95]. Excellent capacitance properties were found by Zhao et al. [63] when working with hydrothermally carbonized tobacco rods. In this work, authors firstly treated the biomass through HTC at 200 °C for 12 h and then activated it at 800 °C for 1 h with a char-to-KOH ratio of 1:3 in mass. Results showed that the activation stage increased the specific surface area up to 2115 $m^2 g^{-1}$, raising significantly also the specific capacitance. Indeed, the produced electrodes showed superb electrical properties with a capacitance as high as 286 and 212 $F g^{-1}$, when the current density was, respectively, 0.5 and 30 $A g^{-1}$. Higher capacitance was recorded when using malva nut as biomass precursor by Ye et al. [96]. HTC was performed at 200 °C for 18 h and hydrochars were further activated at 700 °C in a ratio of 3:1 with KOH. Capacitance up to 279 and 219 $F g^{-1}$ were achieved for current densities of 1 and 20 $A g^{-1}$, respectively. Acid HTC with KOH activation resulted in lower performance when pine cones were used as starting biomass [93]. Manyala et al. tested the addition of 0.5 ml of sulfuric acid into 80 ml of de ionized (DI) water, as medium for the HTC reaction. The further activation was performed for 1 h at the temperatures of 600, 700, 800 and 900 °C, with a KOH-to-char ratio of 1:1 (*w/w*). When temperature reached 900 °C a significant reduction in porosity and electrical properties of the char was observed. This condition is probably due to pore walls collapsing at higher temperature, which enlarge their average dimensions, reducing at the same time the amount of micropores which act as a storage site during charging. A wider inspection of the possible activating agent was conducted by Jain et al. [97] on coconut shells. Biomass was firstly treated in autoclave with H_2O_2 or $ZnCl_2$, testing different dosages and temperatures, and further activated under CO_2 at 800 °C for 2 h. Three different HTC conditions were tested in this work:

1. Temperature of 315 °C, 20 min with a $ZnCl_2$ -to-shell ratio of 1:1 (*w/w*);
2. Temperature of 275 °C, 20 min with a $ZnCl_2$ -to-shell ratio of 3:1 (*w/w*);
3. Temperature of 200 °C, 20 min in a 10% H_2O_2 solution with a successive stage at 275 °C for 20 min with a $ZnCl_2$ -to-shell ratio of 3:1 (*w/w*).

Each set of tests was further proposed under a wide range of biomass concentrations in the solution, ranging from 0.05 to 0.66 $mg L^{-1}$. For the case of $ZnCl_2$ -to-shell ratio of 1:1, authors reported a decrease in the specific surface area as long as biomass concentration was raised, passing from 1700 $m^2 g^{-1}$ for a biomass concentration of 0.05 $mg L^{-1}$, to 1350 $m^2 g^{-1}$ when the concentration was raised to 0.22 $mg L^{-1}$. The tests using H_2O_2 presented a similar trend, with an increase in surface area from 1750 to 2450 $m^2 g^{-1}$ when the biomass concentration was raised from 0.16 to 0.5 $mg L^{-1}$, but a further increase up to 0.66 $mg L^{-1}$ led to an almost 20% reduction in specific surface area. In terms of electrical properties, the highest energy density as well as the highest capacitance was found to be related to carbon produced with H_2O_2 and $ZnCl_2$ with a biomass concentration of 0.5 $mg L^{-1}$, with a capacitance of 246 and 221 $F g^{-1}$ for a current density of 0.25 and 5 $A g^{-1}$, respectively. Impressive performances were also reported in [98] when testing $ZnCl_2$ -activated hydrochar produced from Coca Cola®. Authors found one of the highest capacitances ever recorded for waste precursors, equal to 352.7 $F g^{-1}$ for a current density of 1 $A g^{-1}$. Table 2 summarizes some of the studies reported above with also some reference values for synthetized materials used for supercapacitor applications.

Table 2. Performances of biomass-derived hydrochar for supercapacitors application.

Biomass	HTC Medium	HTC Temp. [°C]	HTC Res. Time [h]	Activation Agent	Activation Temp. [°C]	Activation Time [h]	Max Capacitance [F g ⁻¹]	Ref.
Soybean root	5% H ₂ SO ₄ solution	180	18	KOH	800	3	328 *	[89]
Bamboo shell	1% H ₂ SO ₄ solution	200	24	KOH+ melamine	600–800	1	209 **	[65]
Tobacco rods	H ₂ O	200	12	KOH	800	1	287 **	[63]
Malva nuts	H ₂ O	200	18	KOH	700	1.5	279 *	[96]
Pine cones	1% H ₂ SO ₄ solution	160	12	KOH	600–800	1	78 **	[93]
Self-stacked solvated graphene				-	-	-	245 **	[99]
PANI nanowires through electrochemical deposition				-	-	-	818 **	[100]

* Capacitance calculated at 0.5 A g⁻¹. ** Capacitance calculated at 1 A g⁻¹.

Aside from applications for supercapacitors, hydrochar has been successfully used for the production of electrode material in lithium or sodium ion batteries as well as in the vanadium redox ones [101–104]. In [101], authors used corn stalk as substrate for the production of a bio-based lamellar molybdenum disulfide electrode to be used as anode in a lithium ion battery. To obtain the desired material, a thiourea and ammonium molybdate solution was used as reaction medium for the hydrothermal carbonization of cornstalks. Hydrochars were further treated in a furnace at 1000 °C in N₂ atmosphere and then placed into an ammonium chloride solution at 60 °C, to separate the excess of calcium. The obtained material presented a discharge capacity, after 100 cycles, for a current density of 0.1 and 1 A g⁻¹ of, respectively, 1129 and 339 mAh g⁻¹. A lithium ion battery anode was also produced from a cellulose-derived carbon nanosphere obtained from corn straw by Yu et al. [102]. A sulfuric acid bath and a following sodium hydroxide bath were used to extract cellulose from corn straw. The obtained products were hydrothermally carbonized at 200 °C for 24, 36, 48 and 60 h before being further carbonized at 600 °C in Ar, to obtain carbon nanospheres. Authors found that if reaction time is too long, it can induce particles agglomeration, reducing the available specific area and, therefore, the storage capacity. The best carbonization time was found to be 36 h, which showed a specific discharge capacity after 100 cycles of 577 mA g⁻¹ for a current density of 74 mA g⁻¹. Aside from lithium ion, also applications for sodium ion batteries were studied. In [103], authors tested lath-shaped carbon made through HTC followed by a 800 °C carbonization step produced from peanut shells, to be used as anode in Sodium ion battery. In this case, the discharge capacity was found to be equal to 265 mA g⁻¹ at 30 mA g⁻¹ after 100 cycles. Moreover, tests for a possible cathode material were performed by Palomares et al. [105], using waste from vine shoots and eucalyptus wood as precursor to realize a sodium vanadium fluorophosphate electrode. Authors found that when hydrochar is further subjected to a flash thermal treatment (700 °C, 10 min in N₂), its electrochemical properties reached a specific capacity of more than twofold that of pristine hydrochar.

Promising results were also achieved in vanadium redox flow batteries when testing activated hydrochar [104] as electrode material.

4. Environmental Remediation

4.1. Adsorption of Contaminants

Waste biomass has been widely experimented for the realization of activated carbons for air or water remediation [106]. Indeed, as already seen for the preparation of supercapacitors, biomass can be transformed into a highly carbonaceous porous media, with superior properties in term of specific area and surface composition. Contaminants are adsorbed within the carbon matrix both through physical trapping on the internal surface or chemical bonding on the charged surface of the porous material. Moreover, depending on the characteristics needed for the final material, the HTC treatment and activation step can be further tailored by adjusting the operative parameters.

Two studies involving the use of digestate material as precursor for the realization of activated carbon for the adsorption of contaminants were found in the literature [107,108]. The research conducted by Bernardo et al. [108] on the use of hydrochar from digestate of municipal solid waste, showed a promising perspective for its application on the removal of phosphate from waste water. Digestate was hydrothermally carbonized at 250 °C for 1 h, in acid (with addition of H₂SO₄) or native conditions, before being activated at 600 °C for 2 h with a KOH-to-hydrochar ratio of 3:1 in mass. Despite the reduction in specific surface area when biomass is subjected to acid treatment, the two sets of chars present the same adsorption capacity of 12 mg of orthophosphate for each gram of carbon. Results indicate that morphological properties do not play a significant role in orthophosphate adsorption. According to the authors, the presence of Al³⁺, Ca²⁺, Fe^{2+/3+} and Mg²⁺ ions in the acid hydrochar, can boost the formation of mineral complexes with phosphate ions, reducing its content. Similar behaviors were also reported in [109–111], when operating with bio-chars for the removal of phosphate from aqueous streams.

Hydrochars were also successfully used to remove CO₂ from gaseous streams by using agro-industrial waste or Coca Cola[®] [98,107,112]. Bio chars from agro-industrial waste were produced at different temperatures (190–250 °C), carbonization times (3 and 6 h) and pH levels (5 and 7), in order to evaluate the optimal reaction conditions [107]. Activated carbons were then realized by mixing hydrocarbons (HCs) with KOH in a mass ratio of 1:4 and then heated up to 600 °C for 2 h. Activation considerably boosted surface area and micro-meso porosity of the material. When testing the adsorption capacity, authors found a much greater affinity toward CO₂ than CH₄, with an adsorption capacity of 8.8 mol_{CO2} kg⁻¹, for the carbon produced at 250 °C for 6 h at a pH of 5. Tests on the adsorption of CO₂ were also performed with activated carbons realized from the HTC of garlic peel and Coca Cola[®] [98,112]. Hydrochar from garlic peels [112] were activated under different activation temperatures (600, 700 and 800 °C) and KOH-to-char ratios (0:1; 2:1 and 4:1) in order to investigate their effect on porosity development and adsorption capacity. Tests revealed that an increase in activation temperature and KOH amount led to a rise in specific surface area and pore volume. However, CO₂ adsorption is mainly driven by micropores availability, resulting in lower adsorption capacity as long as temperature and potassium hydroxide increases. Indeed, too severe activation conditions can induce pore enlargement, as well as pore walls collapse, reducing the possible sites for CO₂ immobilization. Superior performances were achieved when using Coca Cola[®] as precursor in the HTC treatment [98]. The work conducted by Boyjoo et al. showed outstanding capacity when Coca Cola[®] was hydrothermally carbonized at 200 °C for 4 h and further activated either with ZnCl₂ or KOH. This latter condition induced the highest increment in the adsorption ability, leading to an adsorption capacity of 5.22 mmol g⁻¹ at 25 °C and 1 Atm, which is one of the highest ever recorded for biomass precursors.

Bernardo et al. produced activated carbon by hydrothermal carbonization of digested sludge and tested their activity toward phosphorous adsorption. They demonstrated that the high porosity together with a high concentration of cations as in Ca, Al, Fe etc., favored phosphates removal from wastewater [108].

Experiments for heavy metals removal were also conducted starting from agro-industrial wastes as reported in [113–115]. In [114], authors tested the removal capacity of Antimony (III) and Cadmium (II) on pyro-char and hydrochar realized from animal manure. The results of the adsorption tests showed higher yields when pyrolytic chars were used, as well as an increase in the removal capacity as long as pH was raised from 3 to 6. The total adsorption potentials for Antimony were 2.24–3.98 and 4.44–16.28 mg g⁻¹, respectively, for hydrochar and pyrochar, while higher capacities were reported for the case of Cadmium, achieving a removal of 19.80–27.18 and 33.48–81.32 mg g⁻¹. Aside from Cadmium removal, promising results on the adsorption of heavy metals contaminants such as lead (Pb) [116,117], copper (Cu) [118–120], Zinc (Zn) [55,113,115] as well as pharmaceutical and chemical waste were obtained in different researches [106,121–124]. For copper removal, different studies proved that surface charge, pH and adsorbent dosage were the main parameters affecting

the adsorption capacity, while for lead superior efficiency (>99.5%) was achieved with Ni/Fe-doped hydrochar [125]. Additionally, organic compounds like methylene blue, methyl orange and Congo red were removed from contaminated solutions through the adsorption on hydrochar produced from biomass waste [126–132]. Up to 655.7 mg of methylene blue for each gram of hydrochar was absorbed when bamboo sawdust was carbonized into 1 M hydrochloric acid solution, before being further treated with NaOH for 1 h. Acid modification led to 100%–200% increase in the adsorption capacity when the solution was kept in the pH range of 10–12 [127].

The removal of Congo red and 2-naphtol was studied by Li et al. in two following works, using bamboo sawdust as starting material [133,134]. Both the two pollutants can have toxic effects on both aquatic life and human organisms and, therefore, need to be removed from the water stream. Moreover, due to their recalcitrant behavior to biological and thermal treatment, the use of adsorbent is more and more studied. In both the studies published by the authors, they found that pore development and the presence of oxygen functional groups on the surface can positively influence the adsorption capacity of the activated carbon. HTC reaction was conducted according to three main procedures: with pure water, with acid medium (HNO₃, H₂SO₄ and H₃PO₄) or through a two-stage operation with a first hydrothermal carbonization in a 5% weight NaOH solution followed by an acid one in HNO₃, H₂SO₄ or H₃PO₄. The two-stage process was used to perform a first delignification in order to favor the penetration of the acid inside the material and enhance pore development. The results showed that, among all, the best adsorption performances were achieved in a two-stage process, with H₂SO₄ or H₃PO₄ as acid medium and were equal to 90.51 and 72.93 mg g⁻¹, respectively, for Congo red and 2-naphtol.

Adsorption of crystal violet (C₂₅H₃₀IN₃) and malachite green was also investigated in biomass-derived hydrochar in [135–137]. For both contaminants, pH represents a key factor for adsorption since it is responsible for the surface charge modification of the hydrochars and the ionic charge modification of the contaminants. It was found that for crystal violet, the optimum pH was 10, while for malachite green it was found to be 7. Food leftovers were also transformed in adsorbent material to remove rare earth ions [138] and toluene [139] from contaminated streams.

Magnetic modified hydrochar, produced from different biomasses through the addition of iron compounds in the reaction media, were also used to remove tetracycline, roxarsone and persistent free radicals from waste water [140–142]. The magnetic properties of the obtained material can reduce the whole purification process time, by shortening the time needed to remove the adsorbent from the solution and saving costs of operation. In Table 3, some of the presented works are reviewed, according to the starting biomass, HTC condition and contaminant removed.

Table 3. Biomass type and HTC condition for removal of contaminants from waste waters.

Biomass	HTC Reaction Conditions	HTC Modifying Agent	Contaminant Removed	Reference
Digestate	250 °C, 1 h	H ₂ SO ₄	Orthophosphate	[108]
Coca Cola®	200 °C, 4 h	KOH, ZnCl ₂	CO ₂	[98]
Animal manure	250 °C	-	Anthimony (III), Cadmium (II)	[114]
Bamboo sawdust	200 °C, 24 h	HCl + NaOH	Methylene blue	[127]

To sum up, the last five years of studies on the possible use of hydrochar material as precursor for the realization of the adsorption of different contaminants, showed interesting potential for the further development of substrates with enhanced capacities that could represent, in the near future, cheaper and more environmentally friendly options with respect to artificially synthesized materials.

4.2. Phosphorous Recovery

Waste biomass as OFMSW and sewage and agro-industrial sludge contain large amounts of phosphorous. Phosphorous (P) is a “critical raw material” for Europe [143] meaning that this element is of strategical importance but reserves of P rock are limited and mostly concentrated in Morocco, USA and China. As stated above, European legislation is pushing and financing for an increase in recovery of P from waste streams [144]. Hydrothermal carbonation of waste biomass, and in particular of sewage sludge containing up to 4% by weight on a dry basis, has demonstrated the possibility of recovering up to 95% of the total phosphorous content [70,145–147]. It has been demonstrated that during HTC, the phosphorous element segregates into the solid phase and treatment of the recovered hydrochar by an acidic leaching leads to the removal of P which moves to the aqueous phase. Phosphorous element in sewage sludge could be found in different forms depending on the reaction conditions [148]. P can be then precipitated by alkalization of the aqueous solution by adding CaO [145] or sodium hydroxide solution [146]. The addition of magnesium chloride and ammonium to the acidic phosphorous solution prior to alkalization led to the precipitation of struvite directly usable as solid fertilizer [146].

4.3. Soil Conditioning

Char addition in soil has been widely recognized as an good practice to favor plant growth, enhancing soil properties in terms of available nutrients, soil porosity and water retention capacity [149–153]. In terms of plant growth, positive outcomes regarding roots nodulation and biomass production were reported in [154,155]. Moreover, different studies demonstrated also the positive effect of hydrochar on the retention of pesticides, allowing an optimized utilization and reducing the possible risk of leakage and contamination of ground waters [156–158]. The fast mineralization of the carbon contained in the char leads to a short-term release of nutrients in the soil, reducing the carbon content by 30–40% within the first 12–19 months [159–161].

The nature of the biomass used to produce the biochar, as well as the operating conditions, can significantly influence the final char composition and, therefore, the possible interaction with the soil [162,163]. A possible drawback of hydrochar addition can be represented by the release of organic compounds that can have toxic effects on soil. To minimize this effect, simple washing, aerobic or low temperature thermal treatment had been reported as further options to reduce the phytotoxic effect of pristine hydrochar [164,165]. Particular attention must be paid also when using HC from sewage sludges, due to the high content and release of heavy metal in the soil [166].

Tests to control ammonia volatilization and optimize nitrogen use for plant growth were proposed in [167–169]. Chu et al. tested the addition of algae-derived hydrochar to increase yield and mitigate N₂O and NH₃ emission [167]. Conversely to the main goal of the work, results showed a significant increase in grain yield up to approximately 25%, together with a rise in N₂O emission and ammonia volatilization. The increased released of nitrogen compounds could be due to the low C/N ratio of the biomass and hydrochar, which could further prompt microbial activities, facilitating nitrogen gasification. Similar results related to emission of N-containing compounds were reported by Subedi et al. [169], as well as by Andert and Mumme [170] when adding pyro or hydro char into soil. On the same aspect, good results with high nitrogen retention, together with a significant decrease in ammonia volatilization was reported in [168] when using acid-modified hydrochar obtained from sewage sludge. Magnesium citrate or magnesium citrate with sulfuric acid were tested as potential additives in the reaction media for the HTC process. In the author’s opinion, the acidity of the chars could reduce the ammonia volatilization, while the high porosity of the carbons can favor the adsorption of NH₄⁺. Moreover, the presence of surface functional groups rich in anion exchange sites can further reduce the nitrification rate, increasing N retention.

Base-modified hydrochars were also successfully tested on the removal of heavy metals like Lead (Pb) and Cadmium (Cd) [171,172]. In [171], authors evaluated the possible addition of 0, 10, 20 and 30% (*w/w*) of lime in the solution, before the HTC treatment. The obtained hydrochars were mixed

with the contaminated soil in a proportion equal to 1, 2.5 and 5% by weight to evaluate the effect on leaching and contaminants immobilization. Results of the trials showed a remarkable increase in the removal of contaminants as long as the share of hydrochar was raised, achieving an improvement in the immobilization efficiency of 95.1% (Pb) and 64.4% (Cd), with respect to pristine hydrochar. Indeed, as long as hydrochar amount and lime content were raised, pH of soil shifted toward basic values, increasing electrostatic interaction between positively charged metals ions and the anions in hydrochar. Moreover, the formation of precipitates like metal (hydr)oxide or carbonate at high soil pH helped to further reduce the amount of Pb and Cd ions in the samples. Copper was also successfully removed from contaminated soil by Xia et al. [172], by using amino-functionalized hydrochar derived from pinewood sawdust. Authors reported an efficiency in Cu removal from the soil equal to 96.2%, together with a reduction of 98.1% in Cu amount in the leachate.

5. Hydrochar for Biorefinery

HTC products were recently proposed, from lab scale up to pilot plant unit, as precursor for the production of many organic compounds that were traditionally synthesized from fossil fuel-derived hydrocarbons [173–176]. Most of the efforts are focused on the production of ethanol, furfural compounds and glucose. During HTC, biomass endures significant modifications leading to the production of a vast amount of different chemical components, both in solid or liquid forms. Ethanol was successfully produced from the cellulose extracted from agave and sugarcane bagasse hydrochar in [177] and [178], achieving a production up to 145 L of ethanol from 1 ton of raw sugarcane bagasse. In order to maximize cellulose production, low temperature HTC (180–190 °C) is preferred. The obtained hydrochar is further treated through enzymatic hydrolysis and fermentation to obtain ethanol. Through the enzymatic hydrolysis of both liquid and solid products of the HTC, glucose was produced from palm oil waste by Zakaria et al. [179].

Furfural and 5-hydroxymethylfurfural (HMF) were also produced from *Miscanthus*, corncob wastes and hemp [180–183]. HMF was successfully generated from both hydrolyzed cellulose or hemicellulose contained in the original biomass. In both cases, acid treatment through H₂SO₄ or catalytic conversion were necessary to produce HMF.

6. Conclusions

HTC represents a valid pre-treatment technology to convert waste biomass into new valuable products which could find applications in a wide range of fields, from energy production to environment remediation and soil conditioning. Since HTC operates in aqueous medium, it is perfectly suitable to convert wet biomass, without any drying step. The most common waste biomass materials include those produced by agro-industries, municipalities (organic fraction of municipal solid waste and sewage sludge) but also from forestry and paper mill industries. The removal of part of the volatile compounds and ashes increases the combustion properties of the hydrochar, making them suitable for direct combustion in energy production applications. Chemical and physical activation, by using KOH or CO₂, respectively, were successfully proposed to increase the surface area and internal porosity of the material. By modifying the morphology and chemical surface, activated hydrochar can be successfully used for the production of energy storage devices for the immobilization of pollutants in gaseous or liquid streams. Pores development as well as elemental and surface composition can be tailored by changing the carbonization and activation parameters. Finally, the addition in soil can induce important benefits on plant growth, increasing water retention and reducing at the same time possible leaching of contaminants into ground water.

Recently, some researchers focused their attention on how to mitigate the energetic impact of the hydrothermal carbonization process by coupling it with renewable energy production systems. Indeed, biochar can represent a valuable product to increase the efficiency of co-digestion systems, with respect to its pristine composition. HC produced from coffee spent, rice straw or microalgae, as well as the liquid phase produced from the hydrothermal carbonization, induced higher biogas

production as well as an increased methane content [184–188]. In such a way, the energy content of the produced biogas can be used to run the HTC reactor, ensuring cleaner combustion with respect to the hydrochar itself. Another option that has recently been studied is to couple the HTC reactor with a solar concentration system which can satisfy the thermal load. Linear parabolic and parabolic disc concentrators ensured a carbonization temperature up to 200 and 250 °C respectively, ensuring heating conditions of traditional systems [189,190].

Nevertheless, there are still some mechanisms in the HTC process that need further study to be completely understood, in order to gain a stronger control over the process parameters, their influence on the final product properties and thus their possible applications. Depending on the HTC operating conditions and the nature of the feedstock, the technology still presents some limitations for its full development. Between them, the correct process liquid treatment and management often present challenges due to the presence of toxic hydrocarbons (such as polycyclic aromatic hydrocarbons (PHAs) and high heavy metals concentrations. The presence of toxic compounds severely limits the possibility to use such residue (as for example in agriculture as a possible source of nutrients) increasing the overall costs of the HTC process. Investigations related to toxic hydrocarbons removal and heavy metals recovery represent a necessary step for further development of the HTC technology.

Author Contributions: Conceptualization, M.P.M., M.V. and A.M.; Writing-Original Draft Preparation, M.P.M.; Writing-Review & Editing, M.P.M., M.V. and A.M.; Supervision & final review, A.M. All authors have read and agreed to the published version of the manuscript.

Funding: This research received no external funding.

Conflicts of Interest: The authors declare no conflict of interest.

References

1. Zhang, B.; Heidari, M.; Regmi, B.; Salaudeen, S.; Arku, P.; Thimmannagari, M.; Dutta, A. Hydrothermal carbonization of fruit wastes: A promising technique for generating hydrochar. *Energies* **2018**, *11*, 2022. [[CrossRef](#)]
2. Volpe, M.; Fiori, L.; Volpe, R.; Messineo, A. Upgrading of olive tree trimmings residue as biofuel by hydrothermal carbonization and torrefaction: A comparative study. In *Chemical Engineering Transactions*; AIDIC: Milan, Italy, 2016; Volume 50, pp. 113–118. ISBN 9788895608419.
3. Lucian, M.; Volpe, M.; Gao, L.; Piro, G.; Goldfarb, J.L.; Fiori, L. Impact of hydrothermal carbonization conditions on the formation of hydrochars and secondary chars from the organic fraction of municipal solid waste. *Fuel* **2018**, *233*, 257–268. [[CrossRef](#)]
4. Arauzo, P.J.; Olszewski, M.P.; Kruse, A. Hydrothermal carbonization brewer's spent grains with the focus on improving the degradation of the feedstock. *Energies* **2018**, *11*, 3226. [[CrossRef](#)]
5. Ferrentino, R.; Ceccato, R.; Marchetti, V.; Andreottola, G. Sewage Sludge Hydrochar: An Option for Removal of Methylene Blue from Wastewater. *Appl. Sci.* **2020**, *10*, 3445. [[CrossRef](#)]
6. Gopu, C.; Gao, L.; Volpe, M.; Fiori, L.; Goldfarb, J.L. Valorizing municipal solid waste: Waste to energy and activated carbons for water treatment via pyrolysis. *J. Anal. Appl. Pyrolysis* **2018**, *133*, 48–58. [[CrossRef](#)]
7. Cavalaglio, G.; Coccia, V.; Cotana, F.; Gelosia, M.; Nicolini, A.; Petrozzi, A. Energy from poultry waste: An Aspen Plus-based approach to the thermo-chemical processes. *Waste Manag.* **2018**, *73*, 496–503. [[CrossRef](#)] [[PubMed](#)]
8. Prins, M.J.; Ptasiński, K.J.; Janssen, F.J.J.G. More efficient biomass gasification via torrefaction. *Energy* **2006**, *31*, 3458–3470. [[CrossRef](#)]
9. Messineo, A.; Ciulla, G.; Messineo, S.; Volpe, M.; Volpe, R. Evaluation of equilibrium moisture content in ligno-cellulosic residues of olive culture. *ARPN J. Eng. Appl. Sci.* **2014**, *9*, 5–11.
10. Heidari, M.; Salaudeen, S.; Norouzi, O.; Acharya, B.; Dutta, A. Numerical comparison of a combined hydrothermal carbonization and anaerobic digestion system with direct combustion of biomass for power production. *Processes* **2020**, *8*, 43. [[CrossRef](#)]
11. Li, H.-Y.; Tsai, G.-L.; Chao, S.-M.; Yen, Y.-F. Measurement of thermal and hydraulic performance of a plate-fin heat sink with a shield. *Exp. Therm. Fluid Sci.* **2012**, *42*, 71–78. [[CrossRef](#)]

12. Ingraio, C.; Bacenetti, J.; Adamczyk, J.; Ferrante, V.; Messineo, A.; Huisingh, D. Investigating energy and environmental issues of agro-biogas derived energy systems: A comprehensive review of Life Cycle Assessments. *Renew. Energy* **2019**, *136*, 296–307. [[CrossRef](#)]
13. Lucian, M.; Fiori, L. Hydrothermal carbonization of waste biomass: Process design, modeling, energy efficiency and cost analysis. *Energies* **2017**, *10*, 211. [[CrossRef](#)]
14. Munir, M.T.; Mansouri, S.S.; Udugama, I.A.; Baroutian, S.; Gernaey, K.V.; Young, B.R. Resource recovery from organic solid waste using hydrothermal processing: Opportunities and challenges. *Renew. Sustain. Energy Rev.* **2018**, *96*, 64–75. [[CrossRef](#)]
15. Álvarez-Murillo, A.; Román, S.; Ledesma, B.; Sabio, E. Study of variables in energy densification of olive stone by hydrothermal carbonization. *J. Anal. Appl. Pyrolysis* **2015**, *113*, 307–314. [[CrossRef](#)]
16. Mäkelä, M.; Benavente, V.; Fullana, A. Hydrothermal carbonization of lignocellulosic biomass: Effect of process conditions on hydrochar properties. *Appl. Energy* **2015**, *155*, 576–584. [[CrossRef](#)]
17. Volpe, M.; Goldfarb, J.L.; Fiori, L. Hydrothermal carbonization of *Opuntia ficus-indica* cladodes: Role of process parameters on hydrochar properties. *Bioresour. Technol.* **2018**, *247*, 310–318. [[CrossRef](#)]
18. Kruse, A.; Funke, A.; Titirici, M.-M. Hydrothermal conversion of biomass to fuels and energetic materials. *Curr. Opin. Chem. Biol.* **2013**, *17*, 515–521. [[CrossRef](#)]
19. Volpe, M.; Wüst, D.; Merzari, F.; Lucian, M.; Andreottola, G.; Kruse, A.; Fiori, L. One stage olive mill waste streams valorisation via hydrothermal carbonisation. *Waste Manag.* **2018**, *80*, 224–234. [[CrossRef](#)]
20. Reza, M.; Lynam, J.G.; Helal Uddin, M.; Coronella, C.J. Hydrothermal carbonization: Fate of inorganics. *Biomass Bioenergy* **2013**, *49*, 86–94. [[CrossRef](#)]
21. Reza, M.T.; Emerson, R.; Uddin, M.H.; Gresham, G.; Coronella, C.J. Ash reduction of corn stover by mild hydrothermal preprocessing. *Biomass Convers. Biorefinery* **2015**, *5*, 21–31. [[CrossRef](#)]
22. Gao, L.; Volpe, M.; Lucian, M.; Fiori, L.; Goldfarb, J.L. Does Hydrothermal Carbonization as a Biomass Pretreatment Reduce Fuel Segregation of Coal-Biomass Blends During Oxidation? *Energy Convers. Manag.* **2019**, *181*, 93–104. [[CrossRef](#)]
23. Smith, A.M.; Singh, S.; Ross, A.B. Fate of inorganic material during hydrothermal carbonisation of biomass: Influence of feedstock on combustion behaviour of hydrochar. *Fuel* **2016**, *169*, 135–145. [[CrossRef](#)]
24. Liu, Z.; Balasubramanian, R. Upgrading of waste biomass by hydrothermal carbonization (HTC) and low temperature pyrolysis (LTP): A comparative evaluation. *Appl. Energy* **2014**, *114*, 857–864. [[CrossRef](#)]
25. Unrean, P.; Lai Fui, B.C.; Rianawati, E.; Acda, M. Comparative techno-economic assessment and environmental impacts of rice husk-to-fuel conversion technologies. *Energy* **2018**, *151*, 581–593. [[CrossRef](#)]
26. Kruse, A.; Koch, F.; Stelzl, K.; Wüst, D.; Zeller, M. Fate of Nitrogen during Hydrothermal Carbonization. *Energy Fuels* **2016**, *30*, 8037–8042. [[CrossRef](#)]
27. Rodriguez Correa, C.; Otto, T.; Kruse, A. Influence of the biomass components on the pore formation of activated carbon. *Biomass Bioenergy* **2017**, *97*, 53–64. [[CrossRef](#)]
28. Liu, F.; Gao, Y.; Zhang, C.; Huang, H.; Yan, C.; Chu, X.; Xu, Z.; Wang, Z.; Zhang, H.; Xiao, X.; et al. Highly microporous carbon with nitrogen-doping derived from natural biowaste for high-performance flexible solid-state supercapacitor. *J. Colloid Interface Sci.* **2019**, *548*, 322–332. [[CrossRef](#)]
29. Yu, X.; Liu, S.; Lin, G.; Yang, Y.; Zhang, S.; Zhao, H.; Zheng, C.; Gao, X. KOH-activated hydrochar with engineered porosity as sustainable adsorbent for volatile organic compounds. *Colloids Surfaces A Physicochem. Eng. Asp.* **2020**, *588*, 124372. [[CrossRef](#)]
30. Hitzl, M.; Corma, A.; Pomares, F.; Renz, M. The hydrothermal carbonization (HTC) plant as a decentral biorefinery for wet biomass. *Catal. Today* **2015**, *257*, 154–159. [[CrossRef](#)]
31. Titirici, M.M. Hydrothermal Carbons: Synthesis, Characterization, and Applications. In *Novel Carbon Adsorbents*; Elsevier: Amsterdam, The Netherlands, 2012; ISBN 9780080977447.
32. Jatzwauck, M.; Schumpe, A. Kinetics of hydrothermal carbonization (HTC) of soft rush. *Biomass Bioenergy* **2015**, *75*, 94–100. [[CrossRef](#)]
33. Volpe, M.; Fiori, L. From olive waste to solid biofuel through hydrothermal carbonisation: The role of temperature and solid load on secondary char formation and hydrochar energy properties. *J. Anal. Appl. Pyrolysis* **2017**, *124*, 63–72. [[CrossRef](#)]
34. Knežević, D.; Van Swaaij, W.; Kersten, S. Hydrothermal conversion of biomass. II. conversion of wood, pyrolysis oil, and glucose in hot compressed water. *Ind. Eng. Chem. Res.* **2010**, *49*, 104–112. [[CrossRef](#)]

35. Kruse, A.; Dahmen, N. Water—A magic solvent for biomass conversion. *J. Supercrit. Fluids* **2015**, *96*, 36–45. [[CrossRef](#)]
36. Sabio, E.; Álvarez-Murillo, A.; Román, S.; Ledesma, B. Conversion of tomato-peel waste into solid fuel by hydrothermal carbonization: Influence of the processing variables. *Waste Manag.* **2016**, *47*, 122–132. [[CrossRef](#)]
37. Heidari, M.; Norouzi, O.; Salaudeen, S.; Acharya, B.; Dutta, A. Prediction of Hydrothermal Carbonization with Respect to the Biomass Components and Severity Factor. *Energy Fuels* **2019**, *33*, 9916–9924. [[CrossRef](#)]
38. Borrero-López, A.M.; Masson, E.; Celzard, A.; Fierro, V. Modelling the reactions of cellulose, hemicellulose and lignin submitted to hydrothermal treatment. *Ind. Crops Prod.* **2018**, *124*, 919–930. [[CrossRef](#)]
39. Mäkelä, M.; Volpe, M.; Volpe, R.; Fiori, L.; Dahl, O. Spatially resolved spectral determination of polysaccharides in hydrothermally carbonized biomass. *Green Chem.* **2018**, *20*, 1114–1120. [[CrossRef](#)]
40. Volpe, M.; Messineo, A.; Mäkelä, M.; Barr, M.R.; Volpe, R.; Corrado, C.; Fiori, L. Reactivity of cellulose during hydrothermal carbonization of lignocellulosic biomass. *Fuel Process. Technol.* **2020**, *206*, 106456. [[CrossRef](#)]
41. Libra, J.A.; Ro, K.S.; Kammann, C.; Funke, A.; Berge, N.D.; Neubauer, Y.; Titirici, M.M.; Fühner, C.; Bens, O.; Kern, J.; et al. Hydrothermal carbonization of biomass residuals: A comparative review of the chemistry, processes and applications of wet and dry pyrolysis. *Biofuels* **2011**, *2*, 71–106. [[CrossRef](#)]
42. Sevilla, M.; Fuertes, A.B. The production of carbon materials by hydrothermal carbonization of cellulose. *Carbon N. Y.* **2009**, *47*, 2281–2289. [[CrossRef](#)]
43. Olszewski, M.P.; Nicolae, S.A.; Arauzo, P.J.; Titirici, M.M.; Kruse, A. Wet and dry? Influence of hydrothermal carbonization on the pyrolysis of spent grains. *J. Clean. Prod.* **2020**, *260*, 121101. [[CrossRef](#)]
44. Kruse, A.; Zevaco, T.A. Properties of hydrochar as function of feedstock, reaction conditions and post-treatment. *Energies* **2018**, *11*, 674. [[CrossRef](#)]
45. Islam, M.A.; Asif, M.; Hameed, B.H. Pyrolysis kinetics of raw and hydrothermally carbonized Karanj (*Pongamia pinnata*) fruit hulls via thermogravimetric analysis. *Bioresour. Technol.* **2015**, *179*, 227–233. [[CrossRef](#)] [[PubMed](#)]
46. Kim, D.; Lee, K.; Park, K.Y. Upgrading the characteristics of biochar from cellulose, lignin, and xylan for solid biofuel production from biomass by hydrothermal carbonization. *J. Ind. Eng. Chem.* **2016**, *42*, 95–100. [[CrossRef](#)]
47. Zhuang, X.; Zhan, H.; Song, Y.; Yin, X.; Wu, C. Structure-reactivity relationships of biowaste-derived hydrochar on subsequent pyrolysis and gasification performance. *Energy Convers. Manag.* **2019**, *199*, 112014. [[CrossRef](#)]
48. Heidari, M.; Dutta, A.; Acharya, B.; Mahmud, S. A review of the current knowledge and challenges of hydrothermal carbonization for biomass conversion. *J. Energy Inst.* **2019**, *92*, 1779–1799. [[CrossRef](#)]
49. Heidari, M.; Salaudeen, S.; Dutta, A.; Acharya, B. Effects of Process Water Recycling and Particle Sizes on Hydrothermal Carbonization of Biomass. *Energy Fuels* **2018**. [[CrossRef](#)]
50. Li, J.; Zhao, P.; Li, T.; Lei, M.; Yan, W.; Ge, S. Pyrolysis behavior of hydrochar from hydrothermal carbonization of pinewood sawdust. *J. Anal. Appl. Pyrolysis* **2020**, *146*, 104771. [[CrossRef](#)]
51. Lucian, M.; Volpe, M.; Fiori, L. Hydrothermal carbonization kinetics of lignocellulosic agro-wastes: Experimental data and modeling. *Energies* **2019**, *12*, 516. [[CrossRef](#)]
52. Ulbrich, M.; Preßl, D.; Fendt, S.; Gaderer, M.; Spliethoff, H. Impact of HTC reaction conditions on the hydrochar properties and CO₂ gasification properties of spent grains. *Fuel Process. Technol.* **2017**, *167*, 663–669. [[CrossRef](#)]
53. Basso, D.; Patuzzi, F.; Castello, D.; Baratieri, M.; Rada, E.C.; Weiss-Hortala, E.; Fiori, L. Agro-industrial waste to solid biofuel through hydrothermal carbonization. *Waste Manag.* **2016**, *47*, 114–121. [[CrossRef](#)] [[PubMed](#)]
54. Zhuang, X.; Song, Y.; Zhan, H.; Yin, X.; Wu, C. Gasification performance of biowaste-derived hydrochar: The properties of products and the conversion processes. *Fuel* **2020**, *260*, 116320. [[CrossRef](#)]
55. Chen, X.; Lin, Q.; He, R.; Zhao, X.; Li, G. Hydrochar production from watermelon peel by hydrothermal carbonization. *Bioresour. Technol.* **2017**, *241*, 236–243. [[CrossRef](#)] [[PubMed](#)]
56. Magdziarz, A.; Wilk, M.; Wądrzyk, M. Pyrolysis of hydrochar derived from biomass—Experimental investigation. *Fuel* **2020**, *167*, 117246. [[CrossRef](#)]
57. Roy, P.; Dutta, A.; Gallant, J. Hydrothermal carbonization of peat moss and herbaceous biomass (*Miscanthus*): A potential route for bioenergy. *Energies* **2018**, *11*, 2794. [[CrossRef](#)]

58. Khatami, R.; Stivers, C.; Joshi, K.; Levendis, Y.A.; Sarofim, A.F. Combustion behavior of single particles from three different coal ranks and from sugar cane bagasse in O₂/N₂ and O₂/CO₂ atmospheres. *Combust. Flame* **2012**, *159*, 1253–1271. [[CrossRef](#)]
59. Wilk, M.; Magdziarz, A.; Kalemba-Rec, I.; Szymańska-Chargot, M. Upgrading of green waste into carbon-rich solid biofuel by hydrothermal carbonization: The effect of process parameters on hydrochar derived from acacia. *Energy* **2020**, *202*, 117717. [[CrossRef](#)]
60. Babinski, B.; Jakab, E.; Sebestyén, Z.; Blazsó, M.; Berényi, B.; Kumar, J.; Krishna, B.B.; Bhaskar, T.; Czégény, Z. Comparison of hydrothermal carbonization and torrefaction of azolla biomass: Analysis of the solid products. *J. Anal. Appl. Pyrolysis* **2020**, 104844. [[CrossRef](#)]
61. Sharma, H.B.; Sarmah, A.K.; Dubey, B. Hydrothermal carbonization of renewable waste biomass for solid biofuel production: A discussion on process mechanism, the influence of process parameters, environmental performance and fuel properties of hydrochar. *Renew. Sustain. Energy Rev.* **2020**, *123*, 109761. [[CrossRef](#)]
62. Zhang, X.; Gao, B.; Zhao, S.; Wu, P.; Han, L.; Liu, X. Optimization of a “coal-like” pelletization technique based on the sustainable biomass fuel of hydrothermal carbonization of wheat straw. *J. Clean. Prod.* **2020**, *242*, 118426. [[CrossRef](#)]
63. Peng, C.; Zhai, Y.; Zhu, Y.; Xu, B.; Wang, T.; Li, C.; Zeng, G. Production of char from sewage sludge employing hydrothermal carbonization: Char properties, combustion behavior and thermal characteristics. *Fuel* **2016**, *176*, 110–118. [[CrossRef](#)]
64. Gunarathne, D.S.; Mueller, A.; Fleck, S.; Kolb, T.; Chmielewski, J.K.; Yang, W.; Blasiak, W. Gasification characteristics of hydrothermal carbonized biomass in an updraft pilot-scale gasifier. *Energy Fuels* **2014**, *28*, 1992–2002. [[CrossRef](#)]
65. Huang, G.; Wang, Y.; Zhang, T.; Wu, X.; Cai, J. High-performance hierarchical N-doped porous carbons from hydrothermally carbonized bamboo shoot shells for symmetric supercapacitors. *J. Taiwan Inst. Chem. Eng.* **2019**, *96*, 672–680. [[CrossRef](#)]
66. Saari, J.; Sermyagina, E.; Kaikko, J.; Vakkilainen, E.; Sergeev, V. Integration of hydrothermal carbonization and a CHP plant: Part 2—Operational and economic analysis. *Energy* **2016**, *113*, 574–585. [[CrossRef](#)]
67. He, C.; Wang, K.; Yang, Y.; Wang, J.Y. Utilization of sewage-sludge-derived hydrochars toward efficient cocombustion with different-rank coals: Effects of subcritical water conversion and blending scenarios. *Energy Fuels* **2014**, *28*, 6140–6150. [[CrossRef](#)]
68. Reza, M.T.; Andert, J.; Wirth, B.; Busch, D.; Pielert, J.; Lynam, J.G.; Mumme, J. Hydrothermal Carbonization of Biomass for Energy and Crop Production. *Appl. Bioenergy* **2014**. [[CrossRef](#)]
69. Saha, N.; Saba, A.; Saha, P.; McGaughey, K.; Franqui-Villanueva, D.; Orts, W.J.; Hart-Cooper, W.M.; Toufiq Reza, M. Hydrothermal carbonization of various paper mill sludges: An observation of solid fuel properties. *Energies* **2019**, *125*, 858. [[CrossRef](#)]
70. Volpe, M.; Fiori, L.; Merzari, F.; Messineo, A.; Andreottola, G. Hydrothermal carbonization as an efficient tool for sewage sludge valorization and phosphorous recovery. *Chem. Eng. Trans.* **2020**, *80*, 199–204. [[CrossRef](#)]
71. Merzari, F.; Goldfarb, J.; Andreottola, G.; Mimmo, T.; Volpe, M.; Fiori, L. Hydrothermal carbonization as a strategy for sewage sludge management: Influence of process withdrawal point on hydrochar properties. *Energies* **2020**, *13*, 2890. [[CrossRef](#)]
72. Wang, R.; Wang, C.; Zhao, Z.; Jia, J.; Jin, Q. Energy recovery from high-ash municipal sewage sludge by hydrothermal carbonization: Fuel characteristics of biosolid products. *Energy* **2019**, *186*, 115848. [[CrossRef](#)]
73. Chen, C.; Liu, G.; An, Q.; Lin, L.; Shang, Y.; Wan, C. From wasted sludge to valuable biochar by low temperature hydrothermal carbonization treatment: Insight into the surface characteristics. *J. Clean. Prod.* **2020**, *263*, 121600. [[CrossRef](#)]
74. Park, K.Y.; Lee, K.; Kim, D. Characterized hydrochar of algal biomass for producing solid fuel through hydrothermal carbonization. *Bioresour. Technol.* **2018**, *258*, 119–124. [[CrossRef](#)] [[PubMed](#)]
75. Saba, A.; McGaughey, K.; Toufiq Reza, M. Techno-economic assessment of co-hydrothermal carbonization of a coal-Miscanthus blend. *Energies* **2019**, *12*, 630. [[CrossRef](#)]
76. Zheng, C.; Ma, X.; Yao, Z.; Chen, X. The properties and combustion behaviors of hydrochars derived from co-hydrothermal carbonization of sewage sludge and food waste. *Bioresour. Technol.* **2019**, *258*, 121347. [[CrossRef](#)] [[PubMed](#)]

77. Wang, T.; Zhai, Y.; Zhu, Y.; Gan, X.; Zheng, L.; Peng, C.; Wang, B.; Li, C.; Zeng, G. Evaluation of the clean characteristics and combustion behavior of hydrochar derived from food waste towards solid biofuel production. *Bioresour. Technol.* **2018**, *266*, 275–283. [[CrossRef](#)]
78. McGaughey, K.; Toufiq Reza, M. Hydrothermal carbonization of food waste: Simplified process simulation model based on experimental results. *Biomass Convers. Biorefinery* **2018**, *8*, 283–292. [[CrossRef](#)]
79. Cao, Z.; Jung, D.; Olszewski, M.P.; Arauzo, P.J.; Kruse, A. Hydrothermal carbonization of biogas digestate: Effect of digestate origin and process conditions. *Waste Manag.* **2019**, *100*, 138–150. [[CrossRef](#)]
80. Pawlak-Kruczek, H.; Sieradzka, M.; Mlonka-Mędrala, A.; Baranowski, M.; Serafin-Tkaczuk, M.; Magdziarz, A.; Niedźwiecki, Ł. Structural and energetic properties of hydrochars obtained from agricultural and municipal solid waste digestates. In Proceedings of the 32nd International Conference on Efficiency, Cost, Optimization, Simulation and Environmental Impact of Energy Systems (ECOS 2019), Wrocław, Poland, 23–28 June 2019.
81. Başakçılardan Kabakçı, S.; Baran, S.S. Hydrothermal carbonization of various lignocellulosics: Fuel characteristics of hydrochars and surface characteristics of activated hydrochars. *Waste Manag.* **2019**, *100*, 259–268. [[CrossRef](#)]
82. Yang, W.; Wang, H.; Zhang, M.; Zhu, J.; Zhou, J.; Wu, S. Fuel properties and combustion kinetics of hydrochar prepared by hydrothermal carbonization of bamboo. *Bioresour. Technol.* **2016**, *205*, 199–204. [[CrossRef](#)]
83. Chen, X.; Ma, X.; Peng, X.; Lin, Y.; Yao, Z. Conversion of sweet potato waste to solid fuel via hydrothermal carbonization. *Bioresour. Technol.* **2018**, *249*, 900–907. [[CrossRef](#)]
84. Celiktas, M.S.; Alptekin, F.M. Conversion of model biomass to carbon-based material with high conductivity by using carbonization. *Energy* **2019**, *188*, 116089. [[CrossRef](#)]
85. Sinan, N.; Unur, E. Hydrothermal conversion of lignocellulosic biomass into high-value energy storage materials. *J. Energy Chem.* **2017**, *26*, 783–789. [[CrossRef](#)]
86. Wang, C.; Wu, D.; Wang, H.; Gao, Z.; Xu, F.; Jiang, K. Biomass derived nitrogen-doped hierarchical porous carbon sheets for supercapacitors with high performance. *J. Colloid Interface Sci.* **2018**, *523*, 133–143. [[CrossRef](#)] [[PubMed](#)]
87. Antero, R.V.P.; Alves, A.C.F.; de Oliveira, S.B.; Ojala, S.A.; Brum, S.S. Challenges and alternatives for the adequacy of hydrothermal carbonization of lignocellulosic biomass in cleaner production systems: A review. *J. Clean. Prod.* **2020**, *252*, 119899. [[CrossRef](#)]
88. Guo, N.; Luo, W.; Guo, R.; Qiu, D.; Zhao, Z.; Wang, L.; Jia, D.; Guo, J. Interconnected and hierarchical porous carbon derived from soybean root for ultrahigh rate supercapacitors. *J. Alloys Compd.* **2020**, *834*, 155115. [[CrossRef](#)]
89. Maniscalco, M.P.; Corrado, C.; Volpe, R.; Messineo, A. Evaluation of the optimal activation parameters for almond shell bio-char production for capacitive deionization. *Bioresour. Technol. Reports* **2020**, *11*, 100435. [[CrossRef](#)]
90. Sevilla, M.; Ferrero, G.A.; Fuertes, A.B. Beyond KOH activation for the synthesis of superactivated carbons from hydrochar. *Carbon N. Y.* **2017**, *114*, 50–58. [[CrossRef](#)]
91. Liu, Y.; An, Z.; Wu, M.; Yuan, A.; Zhao, H.; Zhang, J.; Xu, J. Peony pollen derived nitrogen-doped activated carbon for supercapacitor application. *Chinese Chem. Lett.* **2019**, *31*, 1644–1647. [[CrossRef](#)]
92. Manyala, N.; Bello, A.; Barzegar, F.; Khaleed, A.A.; Momodu, D.Y.; Dangbegnon, J.K. Coniferous pine biomass: A novel insight into sustainable carbon materials for supercapacitors electrode. *Mater. Chem. Phys.* **2016**, *182*, 139–147. [[CrossRef](#)]
93. Zhao, Y.Q.; Lu, M.; Tao, P.Y.; Zhang, Y.J.; Gong, X.T.; Yang, Z.; Zhang, G.Q.; Li, H.L. Hierarchically porous and heteroatom doped carbon derived from tobacco rods for supercapacitors. *J. Power Sources* **2016**, *307*, 391–400. [[CrossRef](#)]
94. Sun, W.; Lipka, S.M.; Swartz, C.; Williams, D.; Yang, F. Hemp-derived activated carbons for supercapacitors. *Carbon N. Y.* **2016**, *103*, 181–192. [[CrossRef](#)]
95. Dai, C.; Wan, J.; Yang, J.; Qu, S.; Jin, T.; Ma, F.; Shao, J. H₃PO₄ solution hydrothermal carbonization combined with KOH activation to prepare argy wormwood-based porous carbon for high-performance supercapacitors. *Appl. Surf. Sci.* **2018**, *444*, 105–117. [[CrossRef](#)]
96. Ye, R.; Cai, J.; Pan, Y.; Qiao, X.; Sun, W. Microporous carbon from malva nut for supercapacitors: Effects of primary carbonizations on structures and performances. *Diam. Relat. Mater.* **2020**, *105*, 107816. [[CrossRef](#)]

97. Jain, A.; Xu, C.; Jayaraman, S.; Balasubramanian, R.; Lee, J.Y.; Srinivasan, M.P. Mesoporous activated carbons with enhanced porosity by optimal hydrothermal pre-treatment of biomass for supercapacitor applications. *Microporous Mesoporous Mater.* **2015**, *218*, 55–61. [[CrossRef](#)]
98. Boyjoo, Y.; Cheng, Y.; Zhong, H.; Tian, H.; Pan, J.; Pareek, V.K.; Jiang, S.P.; Lamonier, J.F.; Jaroniec, M.; Liu, J. From waste Coca Cola® to activated carbons with impressive capabilities for CO₂ adsorption and supercapacitors. *Carbon N. Y.* **2017**, *116*, 490–499. [[CrossRef](#)]
99. Du, P.; Hu, X.; Yi, C.; Liu, H.C.; Liu, P.; Zhang, H.L.; Gong, X. Self-powered electronics by integration of flexible solid-state graphene-based supercapacitors with high performance perovskite hybrid solar cells. *Adv. Funct. Mater.* **2015**, *25*, 2420–2427. [[CrossRef](#)]
100. Gupta, V.; Miura, N. Electrochemically deposited polyaniline nanowire's network a high-performance electrode material for redox supercapacitor. *Electrochem. Solid-State Lett.* **2005**, *8*, A630–A632. [[CrossRef](#)]
101. Zhao, G.; Cheng, Y.; Sun, P.; Ma, W.; Hao, S.; Wang, X.; Xu, X.; Xu, Q.; Liu, M. Biocarbon based template synthesis of uniform lamellar MoS₂ nanoflowers with excellent energy storage performance in lithium-ion battery and supercapacitors. *Electrochim. Acta* **2020**, *331*, 135262. [[CrossRef](#)]
102. Yu, K.; Wang, J.; Song, K.; Wang, X.; Liang, C.; Dou, Y. Hydrothermal synthesis of cellulose-derived carbon nanospheres from corn straw as anode materials for lithium ion batteries. *Nanomaterials* **2019**, *9*, 93. [[CrossRef](#)]
103. Ren, X.; Xu, S.D.; Liu, S.; Chen, L.; Zhang, D.; Qiu, L. Lath-shaped biomass derived hard carbon as anode materials with super rate capability for sodium-ion batteries. *J. Electroanal. Chem.* **2019**, *841*, 63–72. [[CrossRef](#)]
104. Maharjan, M.; Wai, N.; Veksha, A.; Giannis, A.; Lim, T.M.; Lisak, G. Sal wood sawdust derived highly mesoporous carbon as prospective electrode material for vanadium redox flow batteries. *J. Electroanal. Chem.* **2019**, *834*, 94–100. [[CrossRef](#)]
105. Palomares, V.; Blas, M.; Serras, P.; Iturrondobeitia, A.; Peña, A.; Lopez-Urionabarrenechea, A.; Lezama, L.; Rojo, T. Waste Biomass as in Situ Carbon Source for Sodium Vanadium Fluorophosphate/C Cathodes for Na-Ion Batteries. *ACS Sustain. Chem. Eng.* **2018**, *6*, 16386–16398. [[CrossRef](#)]
106. Rodríguez Correa, C.; Ngamying, C.; Klank, D.; Kruse, A. Investigation of the textural and adsorption properties of activated carbon from HTC and pyrolysis carbonizates. *Biomass Convers. Biorefinery* **2018**, *8*, 317–328. [[CrossRef](#)]
107. Rodríguez Correa, C.; Bernardo, M.; Ribeiro, R.P.P.L.; Esteves, I.A.A.C.; Kruse, A. Evaluation of hydrothermal carbonization as a preliminary step for the production of functional materials from biogas digestate. *J. Anal. Appl. Pyrolysis* **2017**, *124*, 461–474. [[CrossRef](#)]
108. Bernardo, M.; Correa, C.R.; Ringelspacher, Y.; Becker, G.C.; Lapa, N.; Fonseca, I.; Esteves, I.A.A.C.; Kruse, A. Porous carbons derived from hydrothermally treated biogas digestate. *Waste Manag.* **2020**, *105*, 170–179. [[CrossRef](#)] [[PubMed](#)]
109. Vikrant, K.; Kim, K.H.; Ok, Y.S.; Tsang, D.C.W.; Tsang, Y.F.; Giri, B.S.; Singh, R.S. Engineered/designer biochar for the removal of phosphate in water and wastewater. *Sci. Total Environ.* **2018**, *616*, 1242–1260. [[CrossRef](#)]
110. Takaya, C.A.; Fletcher, L.A.; Singh, S.; Anyikude, K.U.; Ross, A.B. Phosphate and ammonium sorption capacity of biochar and hydrochar from different wastes. *Chemosphere* **2016**, *145*, 518–527. [[CrossRef](#)]
111. Shepherd, J.G.; Joseph, S.; Sohi, S.P.; Heal, K.V. Biochar and enhanced phosphate capture: Mapping mechanisms to functional properties. *Chemosphere* **2017**, *179*, 57–74. [[CrossRef](#)]
112. Huang, G.G.; Liu, Y.F.; Wu, X.X.; Cai, J.J. Activated carbons prepared by the KOH activation of a hydrochar from garlic peel and their CO₂ adsorption performance. *Xinxing Tan Cailiao/New Carbon Mater.* **2019**, *34*, 247–257. [[CrossRef](#)]
113. Chen, Y.; Chen, J.; Chen, S.; Tian, K.; Jiang, H. Ultra-high capacity and selective immobilization of Pb through crystal growth of hydroxypyromorphite on amino-functionalized hydrochar. *J. Mater. Chem. A* **2015**, *3*, 9843–9850. [[CrossRef](#)]
114. Han, L.; Sun, H.; Ro, K.S.; Sun, K.; Libra, J.A.; Xing, B. Removal of antimony (III) and cadmium (II) from aqueous solution using animal manure-derived hydrochars and pyrochars. *Bioresour. Technol.* **2017**, *234*, 77–85. [[CrossRef](#)] [[PubMed](#)]
115. Sun, K.; Tang, J.; Gong, Y.; Zhang, H. Characterization of potassium hydroxide (KOH) modified hydrochars from different feedstocks for enhanced removal of heavy metals from water. *Environ. Sci. Pollut. Res.* **2015**, *22*, 16640–16651. [[CrossRef](#)] [[PubMed](#)]

116. Zhou, N.; Chen, H.; Xi, J.; Yao, D.; Zhou, Z.; Tian, Y.; Lu, X. Biochars with excellent Pb(II) adsorption property produced from fresh and dehydrated banana peels via hydrothermal carbonization. *Bioresour. Technol.* **2017**, *232*, 204–210. [[CrossRef](#)] [[PubMed](#)]
117. Petrović, J.T.; Stojanović, M.D.; Milojković, J.V.; Petrović, M.S.; Šošarić, T.D.; Laušević, M.D.; Mihajlović, M.L. Alkali modified hydrochar of grape pomace as a perspective adsorbent of Pb²⁺ from aqueous solution. *J. Environ. Manage.* **2016**, *182*, 292–300. [[CrossRef](#)] [[PubMed](#)]
118. Semerciöz, A.S.; Göğüş, F.; Çelekli, A.; Bozkurt, H. Development of carbonaceous material from grapefruit peel with microwave implemented-low temperature hydrothermal carbonization technique for the adsorption of Cu (II). *J. Clean. Prod.* **2017**, *165*, 599–610. [[CrossRef](#)]
119. Deng, J.; Li, X.; Wei, X.; Liu, Y.; Liang, J.; Tang, N.; Song, B.; Chen, X.; Cheng, X. Sulfamic acid modified hydrochar derived from sawdust for removal of benzotriazole and Cu(II) from aqueous solution: Adsorption behavior and mechanism. *Bioresour. Technol.* **2019**, *290*, 121765. [[CrossRef](#)]
120. Zuo, X.J.; Liu, Z.; Chen, M.D. Effect of H₂O₂ concentrations on copper removal using the modified hydrothermal biochar. *Bioresour. Technol.* **2016**, *207*, 262–267. [[CrossRef](#)]
121. Fernandez, M.E.; Ledesma, B.; Román, S.; Bonelli, P.R.; Cukierman, A.L. Development and characterization of activated hydrochars from orange peels as potential adsorbents for emerging organic contaminants. *Bioresour. Technol.* **2015**, *183*, 221–228. [[CrossRef](#)]
122. Lima, H.H.C.; Maniezzo, R.S.; Kupfer, V.L.; Guilherme, M.R.; Moises, M.P.; Arroyo, P.A.; Rinaldi, A.W. Hydrochars based on cigarette butts as a recycled material for the adsorption of pollutants. *J. Environ. Chem. Eng.* **2018**, *6*, 7054–7061. [[CrossRef](#)]
123. Khataee, A.; Kayan, B.; Kalderis, D.; Karimi, A.; Akay, S.; Konsolakis, M. Ultrasound-assisted removal of Acid Red 17 using nanosized Fe₃O₄-loaded coffee waste hydrochar. *Ultrason. Sonochem.* **2017**, *35*, 72–80. [[CrossRef](#)]
124. Khoshbouy, R.; Takahashi, F.; Yoshikawa, K. Preparation of high surface area sludge-based activated hydrochar via hydrothermal carbonization and application in the removal of basic dye. *Environ. Res.* **2019**, *175*, 457–467. [[CrossRef](#)] [[PubMed](#)]
125. Tang, Z.; Deng, Y.; Luo, T.; Xu, Y.; Zhu, N. Enhanced removal of Pb(II) by supported nanoscale Ni/Fe on hydrochar derived from biogas residues. *Chem. Eng. J.* **2016**, *292*, 224–232. [[CrossRef](#)]
126. Buapeth, P.; Watcharin, W.; Dechtrirat, D.; Chuenchom, L. Carbon Adsorbents from Sugarcane Bagasse Prepared through Hydrothermal Carbonization for Adsorption of Methylene Blue: Effect of Heat Treatment on Adsorption Efficiency. *IOP Conf. Ser. Mater. Sci. Eng.* **2019**, *515*, 12003. [[CrossRef](#)]
127. Qian, W.C.; Luo, X.P.; Wang, X.; Guo, M.; Li, B. Removal of methylene blue from aqueous solution by modified bamboo hydrochar. *Ecotoxicol. Environ. Saf.* **2018**, *157*, 300–306. [[CrossRef](#)]
128. Islam, M.A.; Benhouria, A.; Asif, M.; Hameed, B.H. Methylene blue adsorption on factory-rejected tea activated carbon prepared by conjunction of hydrothermal carbonization and sodium hydroxide activation processes. *J. Taiwan Inst. Chem. Eng.* **2015**, *52*, 57–64. [[CrossRef](#)]
129. Fang, J.; Gao, B.; Chen, J.; Zimmerman, A.R. Hydrochars derived from plant biomass under various conditions: Characterization and potential applications and impacts. *Chem. Eng. J.* **2015**, *267*, 253–259. [[CrossRef](#)]
130. Wu, J.; Yang, J.; Feng, P.; Huang, G.; Xu, C.; Lin, B. High-efficiency removal of dyes from wastewater by fully recycling litchi peel biochar. *Chemosphere* **2020**, *246*, 125734. [[CrossRef](#)]
131. Zheng, H.; Sun, Q.; Li, Y.; Du, Q. Biosorbents prepared from pomelo peel by hydrothermal technique and its adsorption properties for congo red. *Mater. Res. Express* **2020**, *7*, 45505. [[CrossRef](#)]
132. Li, B.; Wang, Q.; Guo, J.Z.; Huan, W.W.; Liu, L. Sorption of methyl orange from aqueous solution by protonated amine modified hydrochar. *Bioresour. Technol.* **2018**, *268*, 454–459. [[CrossRef](#)]
133. Li, Y.; Meas, A.; Shan, S.; Yang, R.; Gai, X. Production and optimization of bamboo hydrochars for adsorption of Congo red and 2-naphthol. *Bioresour. Technol.* **2016**, *207*, 379–386. [[CrossRef](#)]
134. Li, Y.; Meas, A.; Shan, S.; Yang, R.; Gai, X.; Wang, H.; Tsend, N. Hydrochars from bamboo sawdust through acid assisted and two-stage hydrothermal carbonization for removal of two organics from aqueous solution. *Bioresour. Technol.* **2018**, *261*, 257–264. [[CrossRef](#)] [[PubMed](#)]
135. Wei, J.; Liu, Y.; Li, J.; Yu, H.; Peng, Y. Removal of organic contaminant by municipal sewage sludge-derived hydrochar: Kinetics, thermodynamics and mechanisms. *Water Sci. Technol.* **2018**, *78*, 947–956. [[CrossRef](#)] [[PubMed](#)]

136. Zhang, H.; Zhang, F.; Huang, Q. Highly effective removal of malachite green from aqueous solution by hydrochar derived from phycocyanin-extracted algal bloom residues through hydrothermal carbonization. *RSC Adv.* **2017**, *7*, 5790–5799. [[CrossRef](#)]
137. Hammud, H.H.; Shmait, A.; Hourani, N. Removal of Malachite Green from water using hydrothermally carbonized pine needles. *RSC Adv.* **2015**, *5*, 7909–7920. [[CrossRef](#)]
138. Feng, Y.; Sun, H.; Han, L.; Xue, L.; Chen, Y.; Yang, L.; Xing, B. Fabrication of hydrochar based on food waste (FWHTC) and its application in aqueous solution rare earth ions adsorptive removal: Process, mechanisms and disposal methodology. *J. Clean. Prod.* **2019**, *212*, 1423–1433. [[CrossRef](#)]
139. Xiao, K.; Liu, H.; Li, Y.; Yang, G.; Wang, Y.; Yao, H. Excellent performance of porous carbon from urea-assisted hydrochar of orange peel for toluene and iodine adsorption. *Chem. Eng. J.* **2020**, *382*, 122997. [[CrossRef](#)]
140. Rattanachueskul, N.; Saning, A.; Kaowphong, S.; Chumha, N.; Chuenchom, L. Magnetic carbon composites with a hierarchical structure for adsorption of tetracycline, prepared from sugarcane bagasse via hydrothermal carbonization coupled with simple heat treatment process. *Bioresour. Technol.* **2017**, *226*, 164–172. [[CrossRef](#)]
141. Zhu, X.; Qian, F.; Liu, Y.; Matera, D.; Wu, G.; Zhang, S.; Chen, J. Controllable synthesis of magnetic carbon composites with high porosity and strong acid resistance from hydrochar for efficient removal of organic pollutants: An overlooked influence. *Carbon N. Y.* **2016**, *99*, 338–347. [[CrossRef](#)]
142. Yu, J.; Zhu, Z.; Zhang, H.; Chen, T.; Qiu, Y.; Xu, Z.; Yin, D. Efficient removal of several estrogens in water by Fe-hydrochar composite and related interactive effect mechanism of H₂O₂ and iron with persistent free radicals from hydrochar of pinewood. *Sci. Total Environ.* **2019**, *658*, 1013–1022. [[CrossRef](#)]
143. European Committee. *EU Report on Critical Raw Materials List*; EC: Brussels, Belgium, 2017.
144. Ava Green Chemistry Development GMBH. *Sewage sludge reuse Phosphate recovery with an innovative HTC technology (HTCycle)*; Ava Green Chemistry Development GMBH: Munich, Germany, 2015.
145. Marin-Batista, J.D.; Mohedano, A.F.; Rodriguez, J.J.; de la Rubia, M.A. Energy and Phosphorous Recovery Through Hydrothermal Carbonization of Digested Sewage Sludge. *Waste Manag.* **2020**, *105*, 566–574. [[CrossRef](#)]
146. Becker, G.C.; Wüst, D.; Köhler, H.; Lautenbach, A.; Kruse, A. Novel approach of phosphate-reclamation as struvite from sewage sludge by utilising hydrothermal carbonization. *J. Environ. Manage.* **2019**, *238*, 119–125. [[CrossRef](#)] [[PubMed](#)]
147. Bhatt, D.; Shrestha, A.; Dahal, R.K.; Acharya, B.; Basu, P.; MacEwen, R. Hydrothermal carbonization of biosolids from Waste water treatment plant. *Energies* **2018**, *11*, 2286. [[CrossRef](#)]
148. Shi, Y.; Luo, G.; Rao, Y.; Chen, H.; Zhang, S. Hydrothermal conversion of dewatered sewage sludge: Focusing on the transformation mechanism and recovery of phosphorus. *Chemosphere* **2019**, *228*, 619–628. [[CrossRef](#)] [[PubMed](#)]
149. Bento, L.R.; Castro, A.J.R.; Moreira, A.B.; Ferreira, O.P.; Bisinoti, M.C.; Melo, C.A. Release of nutrients and organic carbon in different soil types from hydrochar obtained using sugarcane bagasse and vinasse. *Geoderma* **2019**, *334*, 24–32. [[CrossRef](#)]
150. Ji, M.; Sang, W.; Tsang, D.C.W.; Usman, M.; Zhang, S.; Luo, G. Molecular and microbial insights towards understanding the effects of hydrochar on methane emission from paddy soil. *Sci. Total Environ.* **2020**, *714*, 136769. [[CrossRef](#)]
151. Eibisch, N.; Durner, W.; Bechtold, M.; Fuß, R.; Mikutta, R.; Woche, S.K.; Helfrich, M. Does water repellency of pyrochars and hydrochars counter their positive effects on soil hydraulic properties? *Geoderma* **2015**, *245*, 31–39. [[CrossRef](#)]
152. Zhang, S.; Zhu, X.; Zhou, S.; Shang, H.; Luo, J.; Tsang, D.C.W. Hydrothermal carbonization for hydrochar production and its application. In *Biochar from Biomass and Waste: Fundamentals and Applications*; Elsevier: Amsterdam, The Netherlands, 2018; ISBN 9780128117293.
153. Abel, S.; Peters, A.; Trinks, S.; Schonsky, H.; Facklam, M.; Wessolek, G. Impact of biochar and hydrochar addition on water retention and water repellency of sandy soil. *Geoderma* **2013**, *202*, 183–191. [[CrossRef](#)]
154. Scheifele, M.; Hobi, A.; Buegger, F.; Gattinger, A.; Schulin, R.; Boller, T.; Mäder, P. Impact of pyrochar and hydrochar on soybean (*Glycine max* L.) root nodulation and biological nitrogen fixation. *Zeitschrift für Pflanzenernährung und Bodenkunde* **2017**, *180*, 199–211. [[CrossRef](#)]
155. George, E.; Ventura, M.; Panzacchi, P.; Scandellari, F.; Tonon, G. Can hydrochar and pyrochar affect nitrogen uptake and biomass allocation in poplars? *Zeitschrift für Pflanzenernährung und Bodenkunde* **2017**, *180*, 178–186. [[CrossRef](#)]

156. Eibisch, N.; Schroll, R.; Fuß, R. Effect of pyrochar and hydrochar amendments on the mineralization of the herbicide isoproturon in an agricultural soil. *Chemosphere* **2015**, *134*, 528–535. [[CrossRef](#)]
157. Eibisch, N.; Schroll, R.; Fuß, R.; Mikutta, R.; Helfrich, M.; Flessa, H. Pyrochars and hydrochars differently alter the sorption of the herbicide isoproturon in an agricultural soil. *Chemosphere* **2015**, *119*, 155–162. [[CrossRef](#)] [[PubMed](#)]
158. Bera, T.; Purakayastha, T.J.; Patra, A.K.; Datta, S.C. Comparative analysis of physicochemical, nutrient, and spectral properties of agricultural residue biochars as influenced by pyrolysis temperatures. *J. Mater. Cycles Waste Manag.* **2018**. [[CrossRef](#)]
159. Gronwald, M.; Vos, C.; Helfrich, M.; Don, A. Stability of pyrochar and hydrochar in agricultural soil—A new field incubation method. *Geoderma* **2016**, *284*, 85–92. [[CrossRef](#)]
160. Malghani, S.; Jüschke, E.; Baumert, J.; Thuille, A.; Antonietti, M.; Trumbore, S.; Gleixner, G. Carbon sequestration potential of hydrothermal carbonization char (hydrochar) in two contrasting soils; results of a 1-year field study. *Biol. Fertil. Soils* **2015**, *51*, 123–134. [[CrossRef](#)]
161. De Jager, M.; Röhrdanz, M.; Giani, L. The influence of hydrochar from biogas digestate on soil improvement and plant growth aspects. *Biochar* **2020**, *2*, 177–194. [[CrossRef](#)]
162. Yuan, H.; Lu, T.; Wang, Y.; Chen, Y.; Lei, T. Sewage sludge biochar: Nutrient composition and its effect on the leaching of soil nutrients. *Geoderma* **2016**, *267*, 17–23. [[CrossRef](#)]
163. Riedel, T.; Hennessy, P.; Iden, S.C.; Koschinsky, A. Leaching of soil-derived major and trace elements in an arable topsoil after the addition of biochar. *Eur. J. Soil Sci.* **2015**, *66*, 823–834. [[CrossRef](#)]
164. Hitzl, M.; Mendez, A.; Owsianiak, M.; Renz, M. Making hydrochar suitable for agricultural soil: A thermal treatment to remove organic phytotoxic compounds. *J. Environ. Chem. Eng.* **2018**, *6*, 7029–7034. [[CrossRef](#)]
165. Busch, D.; Stark, A.; Kammann, C.I.; Glaser, B. Genotoxic and phytotoxic risk assessment of fresh and treated hydrochar from hydrothermal carbonization compared to biochar from pyrolysis. *Ecotoxicol. Environ. Saf.* **2013**, *97*, 59–66. [[CrossRef](#)]
166. Yue, Y.; Yao, Y.; Lin, Q.; Li, G.; Zhao, X. The change of heavy metals fractions during hydrochar decomposition in soils amended with different municipal sewage sludge hydrochars. *J. Soils Sediments* **2017**, *17*, 763–770. [[CrossRef](#)]
167. Chu, Q.; Xue, L.; Cheng, Y.; Liu, Y.; Feng, Y.; Yu, S.; Meng, L.; Pan, G.; Hou, P.; Duan, J.; et al. Microalgae-derived hydrochar application on rice paddy soil: Higher rice yield but increased gaseous nitrogen loss. *Sci. Total Environ.* **2020**, *717*, 137127. [[CrossRef](#)] [[PubMed](#)]
168. Chu, Q.; Xue, L.; Singh, B.P.; Yu, S.; Müller, K.; Wang, H.; Feng, Y.; Pan, G.; Zheng, X.; Yang, L. Sewage sludge-derived hydrochar that inhibits ammonia volatilization, improves soil nitrogen retention and rice nitrogen utilization. *Chemosphere* **2020**, *245*, 125558. [[CrossRef](#)] [[PubMed](#)]
169. Subedi, R.; Kammann, C.; Pelissetti, S.; Taupe, N.; Bertora, C.; Monaco, S.; Grignani, C. Does soil amended with biochar and hydrochar reduce ammonia emissions following the application of pig slurry? *Eur. J. Soil Sci.* **2015**, *66*, 1044–1053. [[CrossRef](#)]
170. Andert, J.; Mumme, J. Impact of pyrolysis and hydrothermal biochar on gas-emitting activity of soil microorganisms and bacterial and archaeal community composition. *Appl. Soil Ecol.* **2015**, *96*, 225–239. [[CrossRef](#)]
171. Xia, Y.; Liu, H.; Guo, Y.; Liu, Z.; Jiao, W. Immobilization of heavy metals in contaminated soils by modified hydrochar: Efficiency, risk assessment and potential mechanisms. *Sci. Total Environ.* **2019**, *685*, 1201–1208. [[CrossRef](#)] [[PubMed](#)]
172. Xia, Y.; Luo, H.; Li, D.; Chen, Z.; Yang, S.; Liu, Z.; Yang, T.; Gai, C. Efficient immobilization of toxic heavy metals in multi-contaminated agricultural soils by amino-functionalized hydrochar: Performance, plant responses and immobilization mechanisms. *Environ. Pollut.* **2020**, *261*, 114217. [[CrossRef](#)]
173. Du, F.L.; Du, Q.S.; Dai, J.; Tang, P.D.; Li, Y.M.; Long, S.Y.; Xie, N.Z.; Wang, Q.Y.; Huang, R.B. A comparative study for the organic byproducts from hydrothermal carbonizations of sugarcane bagasse and its bio-refined components cellulose and lignin. *PLoS ONE* **2018**, *13*, e0197188. [[CrossRef](#)]
174. Chang, M.Y.; Huang, W.J. Hydrothermal biorefinery of spent agricultural biomass into value-added bio-nutrient solution: Comparison between greenhouse and field cropping data. *Ind. Crops Prod.* **2018**, *126*, 186–189. [[CrossRef](#)]

175. Ruiz, H.A.; Conrad, M.; Sun, S.N.; Sanchez, A.; Rocha, G.J.M.; Romani, A.; Castro, E.; Torres, A.; Rodríguez-Jasso, R.M.; Andrade, L.P.; et al. Engineering aspects of hydrothermal pretreatment: From batch to continuous operation, scale-up and pilot reactor under biorefinery concept. *Bioresour. Technol.* **2020**, *299*, 122685. [[CrossRef](#)]
176. Ashraf, M.T.; Schmidt, J.E. Process simulation and economic assessment of hydrothermal pretreatment and enzymatic hydrolysis of multi-feedstock lignocellulose—Separate vs combined processing. *Bioresour. Technol.* **2018**, *249*, 835–843. [[CrossRef](#)]
177. Aguilar, D.L.; Rodríguez-Jasso, R.M.; Zanuso, E.; de Rodríguez, D.J.; Amaya-Delgado, L.; Sanchez, A.; Ruiz, H.A. Scale-up and evaluation of hydrothermal pretreatment in isothermal and non-isothermal regimen for bioethanol production using agave bagasse. *Bioresour. Technol.* **2018**, *263*, 112–119. [[CrossRef](#)] [[PubMed](#)]
178. Nascimento, V.M.; Rossell, C.E.V.; de Moraes Rocha, G.J. Scale-up hydrothermal pretreatment of sugarcane bagasse and straw for second-generation ethanol production. In *Hydrothermal Processing in Biorefineries: Production of Bioethanol and High Added-Value Compounds of Second and Third Generation Biomass*; Springer: New York, NY, USA, 2017; ISBN 9783319564579.
179. Zakaria, M.R.; Hirata, S.; Hassan, M.A. Hydrothermal pretreatment enhanced enzymatic hydrolysis and glucose production from oil palm biomass. *Bioresour. Technol.* **2015**, *176*, 142–148. [[CrossRef](#)] [[PubMed](#)]
180. Rivas, S.; Vila, C.; Alonso, J.L.; Santos, V.; Parajó, J.C.; Leahy, J.J. Biorefinery processes for the valorization of Miscanthus polysaccharides: From constituent sugars to platform chemicals. *Ind. Crops Prod.* **2019**, *134*, 309–317. [[CrossRef](#)]
181. Deng, A.; Ren, J.; Li, H.; Peng, F.; Sun, R. Corn cob lignocellulose for the production of furfural by hydrothermal pretreatment and heterogeneous catalytic process. *RSC Adv.* **2015**, *5*, 60264–60272. [[CrossRef](#)]
182. Li, H.; Wang, X.; Liu, C.; Ren, J.; Zhao, X.; Sun, R.; Wu, A. An efficient pretreatment for the selectively hydrothermal conversion of corn cob into furfural: The combined mixed ball milling and ultrasonic pretreatments. *Ind. Crops Prod.* **2016**, *94*, 721–728. [[CrossRef](#)]
183. Paze, A.; Brazdauskas, P.; Rizhikovs, J.; Puke, M.; Tupciauskas, R.; Andzs, M.; Meile, K.; Vedernikovs, N. Changes in the Polysaccharide Complex of Lignocellulose after Catalytic Hydrothermal Pre-Treatment Process of Hemp (*Cannabis Sativa* L.) Shives. In Proceedings of the 23th European Biomass Conference and Exhibition, Vienna, Austria, 1–4 June 2015; pp. 1063–1069. [[CrossRef](#)]
184. Codignole Luz, F.; Volpe, M.; Fiori, L.; Manni, A.; Cordiner, S.; Mulone, V.; Rocco, V. Spent coffee enhanced biomethane potential via an integrated hydrothermal carbonization-anaerobic digestion process. *Bioresour. Technol.* **2018**, *256*, 102–109. [[CrossRef](#)]
185. Passos, F.; Ferrer, I. Influence of hydrothermal pretreatment on microalgal biomass anaerobic digestion and bioenergy production. *Water Res.* **2015**, *68*, 364–373. [[CrossRef](#)]
186. Weide, T.; Brüggling, E.; Wetter, C. Anaerobic and aerobic degradation of wastewater from hydrothermal carbonization (HTC) in a continuous, three-stage and semi-industrial system. *J. Environ. Chem. Eng.* **2019**, *7*, 102912. [[CrossRef](#)]
187. He, L.; Huang, H.; Zhang, Z.; Lei, Z.; Lin, B. Le Energy Recovery from Rice Straw through Hydrothermal Pretreatment and Subsequent Biomethane Production. *Energy Fuels* **2017**, *31*, 10850–10857. [[CrossRef](#)]
188. Lucian, M.; Volpe, M.; Merzari, F.; Wüst, D.; Kruse, A.; Andreottola, G.; Fiori, L. Hydrothermal carbonization coupled with anaerobic digestion for the valorization of the organic fraction of municipal solid waste. *Bioresour. Technol.* **2020**, *314*, 123734. [[CrossRef](#)]
189. Ischia, G.; Orlandi, M.; Fendrich, M.A.; Bettonte, M.; Merzari, F.; Miotello, A.; Fiori, L. Realization of a solar hydrothermal carbonization reactor: A zero-energy technology for waste biomass valorization. *J. Environ. Manage.* **2020**, *259*, 110067. [[CrossRef](#)] [[PubMed](#)]
190. Xiao, C.; Liao, Q.; Fu, Q.; Huang, Y.; Chen, H.; Zhang, H.; Xia, A.; Zhu, X.; Reungsang, A.; Liu, Z. A solar-driven continuous hydrothermal pretreatment system for biomethane production from microalgae biomass. *Appl. Energy* **2019**, *236*, 1011–1018. [[CrossRef](#)]

